R/D - 5878-CH-01-2

(2)

UNIVERSITY OF NOTTINGHAM

DEPARTMENT OF CHEMISTRY

Corrosion of Aluminium Alloys by IRFNA

R & D 5878-CH-01

M F A Dove
N Logan
J P Mauger
J F Richings

SECOND INTERIM REPORT
JULY 1988

CONTENTS

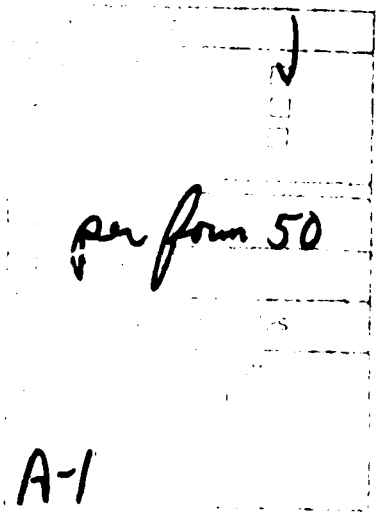

1) INTRODUCTION

This second interim report presents the results of work carried out under the revised agreements of March 1988 between Dr. Barry Allan (USAMC) and Drs. N.Logan and M.F.A.Dove (University of Nottingham, Department of Inorganic Chemistry). The agreement outlined five areas of research which can be summarised as follows:

A) An investigation into the relative corrosivity of various samples of IRFNA upon aluminium alloys , using electrochemical monitoring of both corrosion potential (E_{corr}), and polarisation-resistance, R_p (and hence corrosion rates) with time.

B) The effect of altering working electrode environment by cell rotation upon the corrosion behaviour of aluminium alloys in IRFNA : specifically, the change in corrosion rate of an alloy sample as it is moved from an ullage-space environment to a liquid-phase environment.

C) The effects of temperature cycling upon the rates of corrosion of aluminium alloy in IRFNA.

D) An investigation into the effects of surface pretreatment and exposure to IRFNA of samples of 3L65 alloy using Auger spectroscopy.

E) The effects of water and/or dissolved metal ions upon the rate of corrosion of aluminium alloy in IRFNA.

Further to these proposed areas of study, it was agreed to analyse

samples of IRFNA for:

i) total solids content

ii) HF content

iii) H_2O content

iv) metals content (Al, Fe, Cu)

2) RESEARCH AREAS

2.1) PART A - ELECTROLYTE EFFECTS

Concern has been expressed that IRFNA procured from different sources of supply, and hence containing different levels of water, HF, dissolved solids, etc., may produce varying rates of corrosion of storage tank alloys. In order to assess the effects of these variables upon the corrosion rate of aluminium alloy in IRFNA, four pairs of electrochemical cells, of the bottom working electrode type (Fig. 1a), machined from 3L65 alloy and containing working electrodes cut from SN5144 oxidiser tank wall section, were constructed. The SN5144 oxidiser tank wall section used for the fabrication of these working electrodes was selected arbitrarily, i.e. without recognition of the left hand (LH) or right hand (RH) designation used previously, since no significant difference in corrosion behaviour was observed for such LH or RH samples in the previous studies (ref. 2). Each pair of cells was filled with IRFNA obtained from different sources. The cells were placed in a thermostatted oil-bath maintained at 25°C, and at convenient times, corrosion potential (E_{corr}) and polarisation resistance (R_p), were measured. Corrosion current densities (i_{corr}) were obtained in the usual manner.

Table 2.1 shows cell codes, IRFNA-type and set-up dates for the four pairs of cells. Figures 2 to 5 show the variation of corrosion

FIG. 1a The Bottom Working-electrode Cell

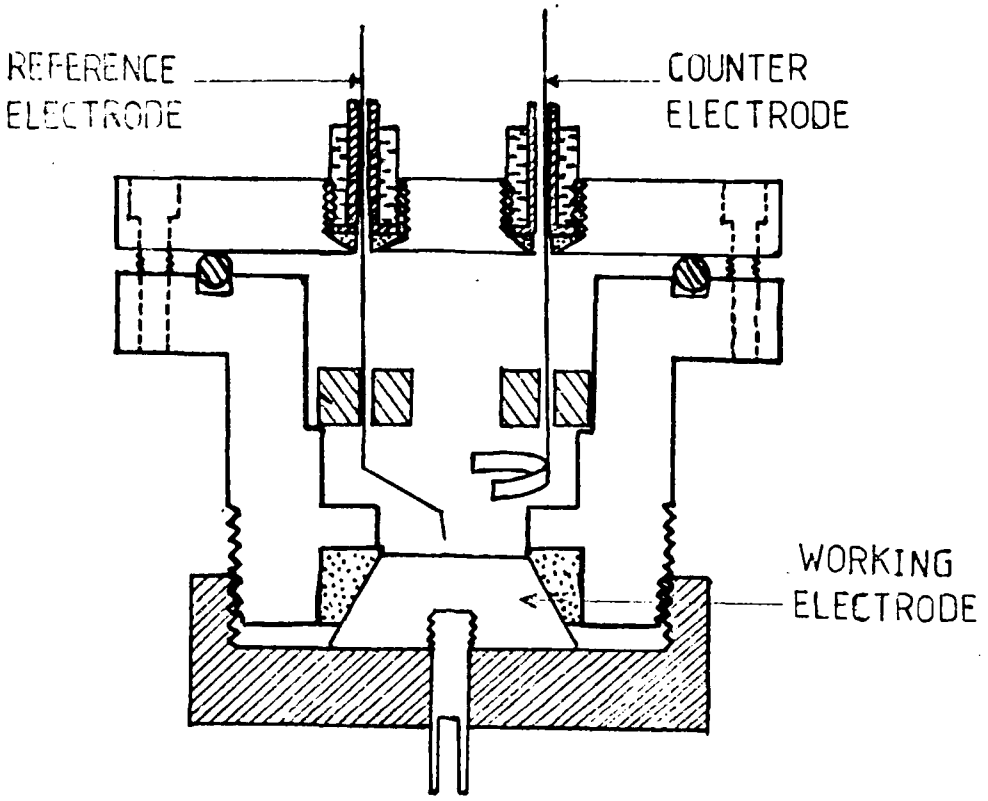

NYLON

TEFLON

KEL-F

BRASS

potential with time. Figures 6 to 9 illustrate the changes in corrosion current density with time.

TABLE 2.1: Cell types used in part A

Cell Code	IRFNA Type	Weight of Electrolyte / g	Set-up date
Boom 1	Boom	13.728	13-4-88
Boom 2	Boom	12.069	14-4-88
AF058/1	AF058	13.454	28-4-88
AF058/2	AF058	13.403	28-4-88
SN/1	SN5208	13.943	20-5-88
SN/2	SN5208	14.398	20-5-88
W1	Westcott	12.141	20-6-88
W2	lot67 drum3	13.972	24-6-88

The results are presented and discussed in Section 3.1.

2.2) PART B - THE FOUR WORKING-ELECTRODE CELL

In order to investigate the effects of electrode orientation upon the rate of corrosion, an electrochemical cell containing four working-electrodes has been constructed (Fig. 1b).

The cell consists of a block of H30 aluminium alloy bored out to an internal diameter of 52.6mm and depth of 69.07mm. Working electrodes (11.5mm diameter) cut from SN5144 oxidiser tank wall section are positioned at 0°,90°,180° and 270° around the internal walls and are insulated from the cell body by Kel-F seals. Platinum reference and counter electrodes are inserted through Kel-F seals in the cell body and lid respectively. The cell has a surface-to-volume ratio of ca. 1.08cm^{-1}, and was filled with IRFNA (87g, supplied by R.O.Westcott (Lot 67 Drum 3)) on 18-2-88. The cell was placed in a thermostatically controlled oil-bath maintained at a temperature of 25°C.

The corrosion potential and polarisation resistance of the four working-electrodes were recorded with the cell orientated such that three of the working electrodes (WE1, WE2 and WE3) were fully immersed in electrolyte (IRFNA), with the fourth working electrode (WE4) in ullage space. After a period of ca. 69 days the cell was rotated through 90° with the result that WE3 was moved from a liquid-phase environment to the ullage space and WE4 was moved from the ullage space to the liquid phase. During this changeover period the corrosion potential was recorded

Figure 1b

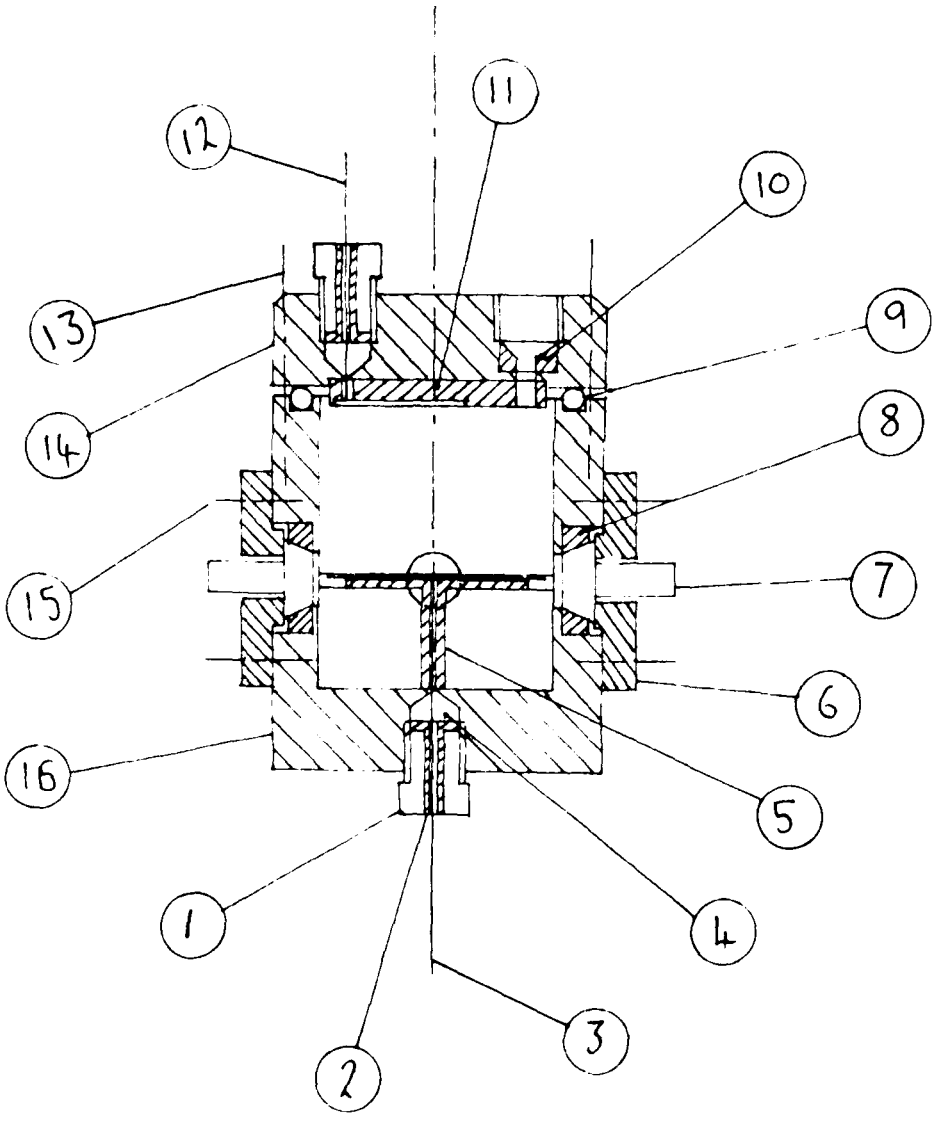

PART Nº	NAME OF PART	Nº OF PARTS
16	ALUMINIUM BODY	1
15	M3 STAINLESS STEEL SCREW	16
14	ALUMINIUM LID	1
13	M4 STAINLESS STEEL SCREW	4
12	COUNTER ELECTRODE	1
11	PTFE COUNTER ELECTRODE GUIDE	1
10	PTFE VALVE SEAT	1
9	PTFE 'O'RING	1
8	KEL-F SEALING RING	4
7	WORKING ELECTRODE	4
6	NYLON CLAMPING RING	4
5	PTFE ELECTRODE GUIDE	1
4	KEL-F ELECTRODE SEATS	2
3	CRUCIFORM REFERENCE ELECTRODE	1
2	NYLON INSULATING INSERT	2
1	BRASS ELECTRODE BOLT	2

OTTINGHAM UNIVERSITY | THE FOUR WORKING-ELECTRODE CELL | SCALE 1:1 | MATERIAL : ALUMINIUM HE30 GRADE

at frequent intervals.

The results are presented and discussed in Section 3.2.

2.3) PART C - TEMPERATURE CYCLING

In the previous report (ref. 1) the effect of oscillating temperature cycles on the corrosion rate of aluminium alloy in IRFNA was described. Two bottom working electrode cells , BW13 and BW14 (water washed and dried), were transferred to a temperature oscillation bath (at 25°C). The temperature of the bath was oscillated by ±5°C over a 24 hour period. E_{corr} and i_{corr} were recorded at regular intervals during the cycle.

Two more bottom working electrode cells, BW1 and BW2B (no pretreatment), were transferred to the temperature oscillation bath on the 12th April 1988. The histories of the cells prior to this date are shown in Table 2.2.

TABLE 2.2: Cell histories

Cell Code	Electrode Type	Pretreatment	IRFNA Supply	Duration
BW1	LH	No pretreatment	R.O.Westcott	628.2 days
BW2B	RH	"	"	589.2 days

The temperature of the bath was oscillated by ±20°C over a 24 hour period. E_{corr} and i_{corr} measurements were determined for all four cells at intervals during the cycle. The results of these

experiments are presented and discussed in Section 3.3.

2.4) PART D - SURFACE PRETREATMENT

The proposal is to study five pairs of samples cut from oxidiser tank SN5144. The pretreatments agreed are as follows:

1) No pretreatment

2) H_2O wash, dry

3) H_2O wash, dry, IRFNA (3 months)

4) H_2O wash, dry, HF/F_2

5) H_2O wash, dry, HF/F_2, IRFNA (3months)

For sample pairs 3 and 5, the final stage of pretreatment involving immersion in IRFNA (R.O. Westcott Lot67 Drum3) was commenced on 25 May 1988. All the samples will be characterised using the Auger facility at Loughborough Consultants Ltd. when the three month exposure period of these two pairs of samples is complete.

2.5) PART E - " DOPING "

Since a great deal of emphasis had been placed upon the effect of either increased water and/or dissolved metal ions content in IRFNA, this part of the proposal was designed to investigate these variables.

The presence of water in IRFNA at concentrations greater than allowed for by specification limits is expected to increase significantly the rate of corrosion of aluminium alloys in this medium. With this in mind, it was proposed to determine the water content of the various IRFNA samples available to us, and then to increase the water content of one of those samples to a known level above the upper specification limit (2.5 wt.% ref. 4) and to measure the corrosion rate of the SN5144 alloy in this "water-doped" acid.

However, in order to avoid the long "induction" periods associated with these electrochemical systems (up to 80 days), it was decided to inject doped RFNA into cells which had been running for some time.

As the effects of the dissolved metal content on the corrosion rates of alloys in IRFNA are unknown, it was proposed to investigate these by doping RFNA samples (prepared in our laboratory), and injecting the doped acids into electrochemical cells which had been running for some time and had achieved a steady corrosion rate.

2.6) IRFNA ANALYSES

In order to interpret the results obtained from parts A and E, it is necessary to know the composition of the acid electrolyte present in the electrochemical cells, particularly HF, H_2O, total solids and metals contents.

Results of sample analyses are reported in Section 3.6.

3) RESULTS AND DISCUSSION

3.1) PART A - ELECTROLYTE EFFECTS

3.1.1) Potential-Time Behaviour

Figures 2 to 5 show the variation of corrosion potential (E_{corr}) with time of the four pairs of electrochemical cells. Typical E_{corr}-time curves are obtained from Boom 1 and Boom 2 cells (Figure 2). In these cases the cell potential falls to a value of ca. -820mV after a period of ca. 50 days. This behaviour has been observed and reported previously (ref. 2), and is associated with the fluoride film present on the surface of these working electrodes cut from oxidiser tank wall sections. Indeed, working electrodes which have had the fluoride film removed (cells BW5,BW6,BW7 and BW8 - ref. 2) show a much lower rate of fall of potential to the value of ca. -820mV (> 150 days) than electrodes covered by the fluoride film.

The cells W1 and W2, containing IRFNA supplied by R.O. Westcott, show a very rapid fall to low corrosion potentials (Figure 5). Similar behaviour is observed in the pair of cells filled with SN5208 IRFNA (Figure 4). The observed behaviour is very similar to that reported in ref. 2 for cell pairs BW23 / BW24 and BW21 / BW22. Again a fluoride-film is present on the working electrodes.

The results obtained for cells AF058/1 and AF058/2 (Figure 3)

Figure 2 : Boom 1 (•) and Boom 2 (o) : E_{corr} vs. time

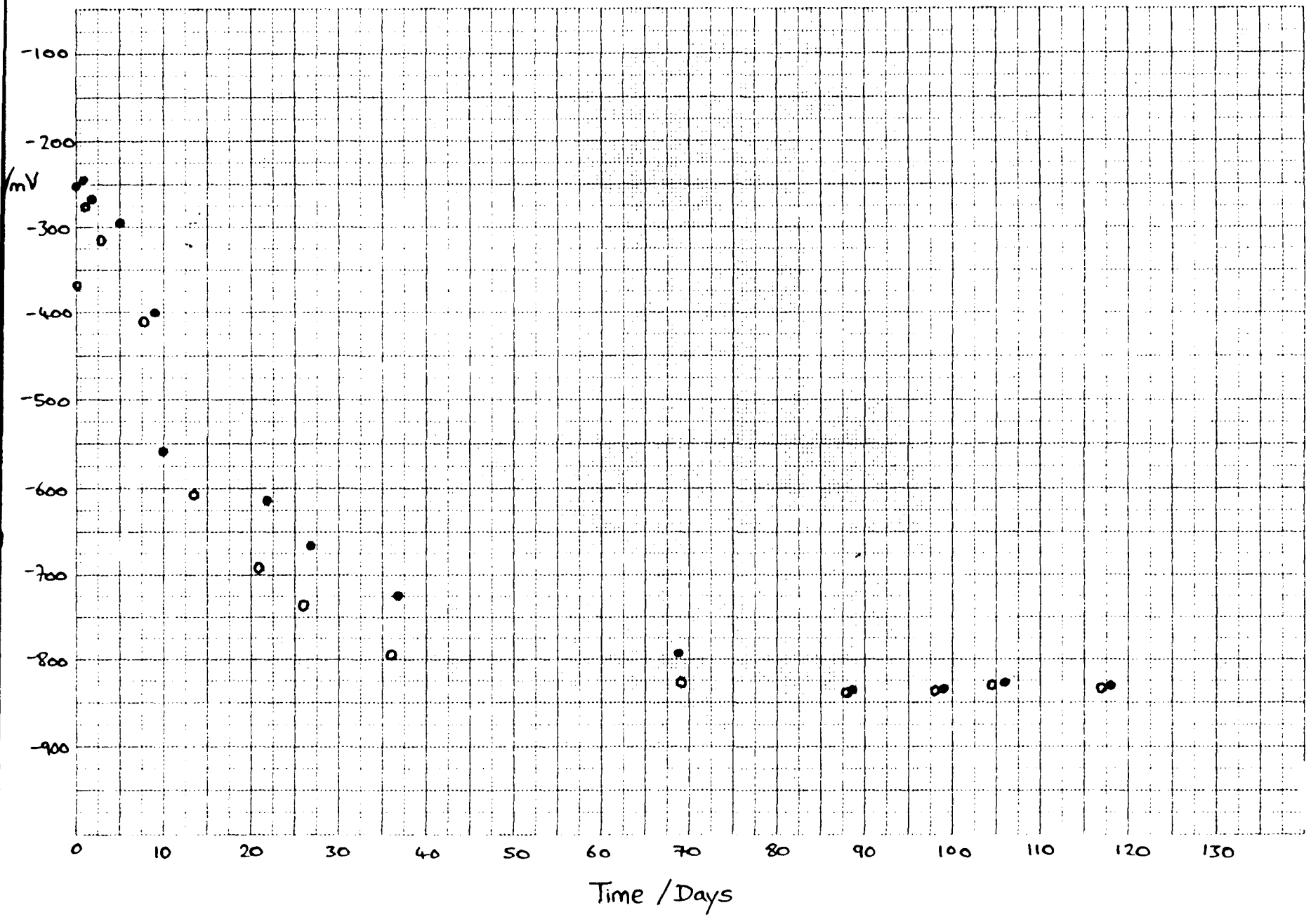

Figure 3 : AF058/1 (●) and AF058/2 (o) : Ecorr vs. time

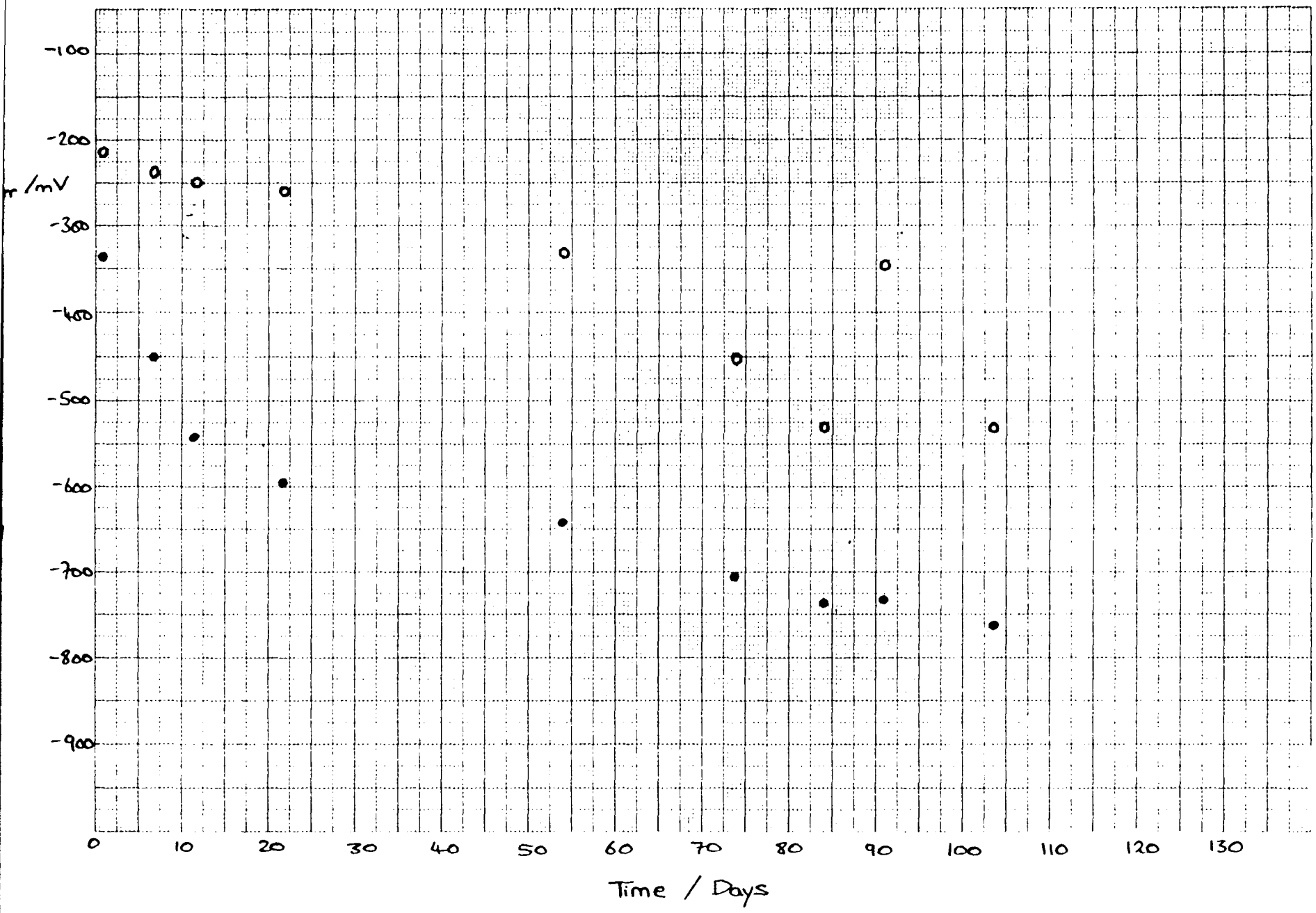

Figure 4 : SN5208/1 (●) and SN5208/2 (○) : E_{corr} vs. time

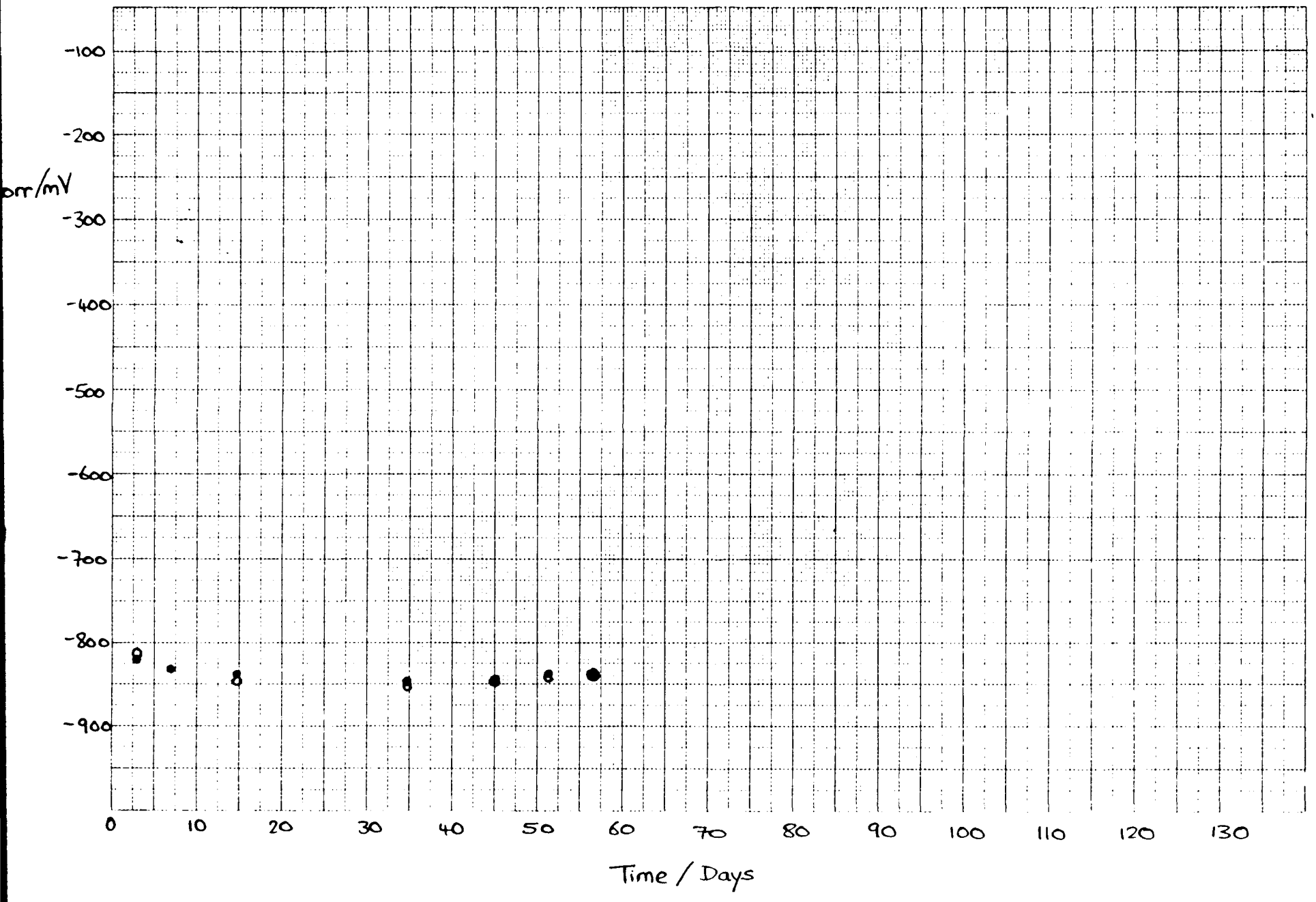

Figure 5 : W1 (•) and W2 (o) : Ecorr vs. time

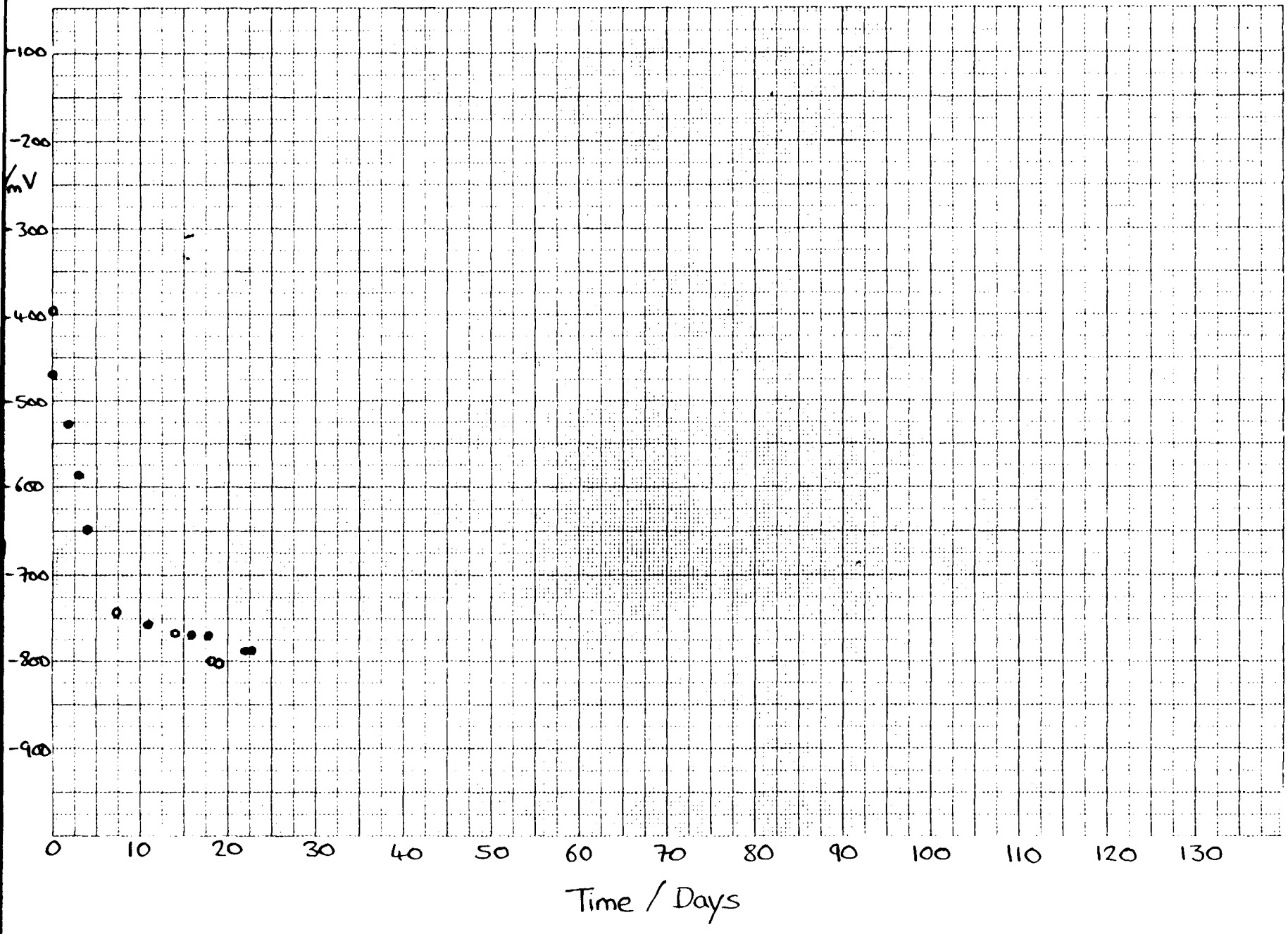

show markedly different behaviour. The most obvious difference between E_{corr}-time data for these cells and those reported above is the much slower rate of fall of working electrode potential of the AF058 cells. At times of ca. 84 days, working electrode potentials were -735mV and -530mV respectively for AF058/1 and AF058/2. The working electrodes of this pair of cells are of the same type as those of the other cells discussed here (SN5144 oxidiser tank wall sections), and so are also covered with the fluoride film . Figure 3 also illustrates the diference in potential-time behaviour of the two AF058 cells. Cell AF058/1 shows a potential-time curve similar to the typical behaviour displayed by Boom1 and Boom2, although after 50 days the working electrode potential has fallen to only ca. -640mV (cf. ca. -800mV for BW1/2). Cell AF058/2 shows potential-time behaviour more typical of bare, untreated 3L65 aluminium alloy when exposed to IRFNA (ref. 2, Figs. 13 and 14: BW21, BW22, BW23 and BW24 cell-wall E_{corr} versus time data).

3.1.2 Corrosion current density - Time behaviour

Figures 6 to 9 display corrosion current density (i_{corr})versus time data for the four pairs of electrochemical cells used in this part of the programme. Values of i_{corr} were calculated in the usual manner from polarisation-resistance (R_p) data.

All data obtained up to the present time indicate electrode behaviour similar to that which has been reported previously (ref. 2).

Figure 6 : Boom 1 (•) and Boom 2 (o): i_{corr} vs. time

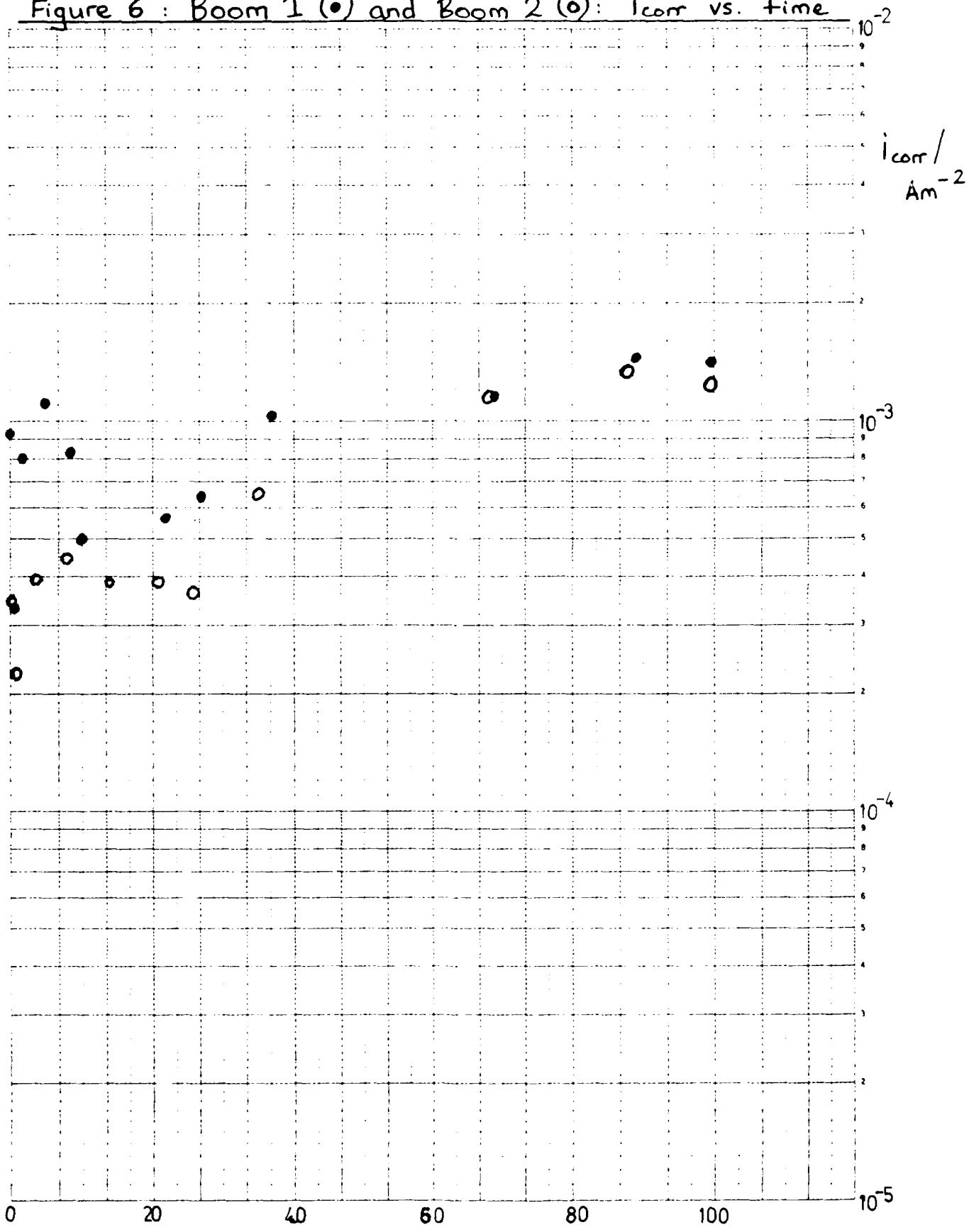

Figure 7 : SN5208/1 (•) and SN5208/2 (o) i_{corr} vs. time

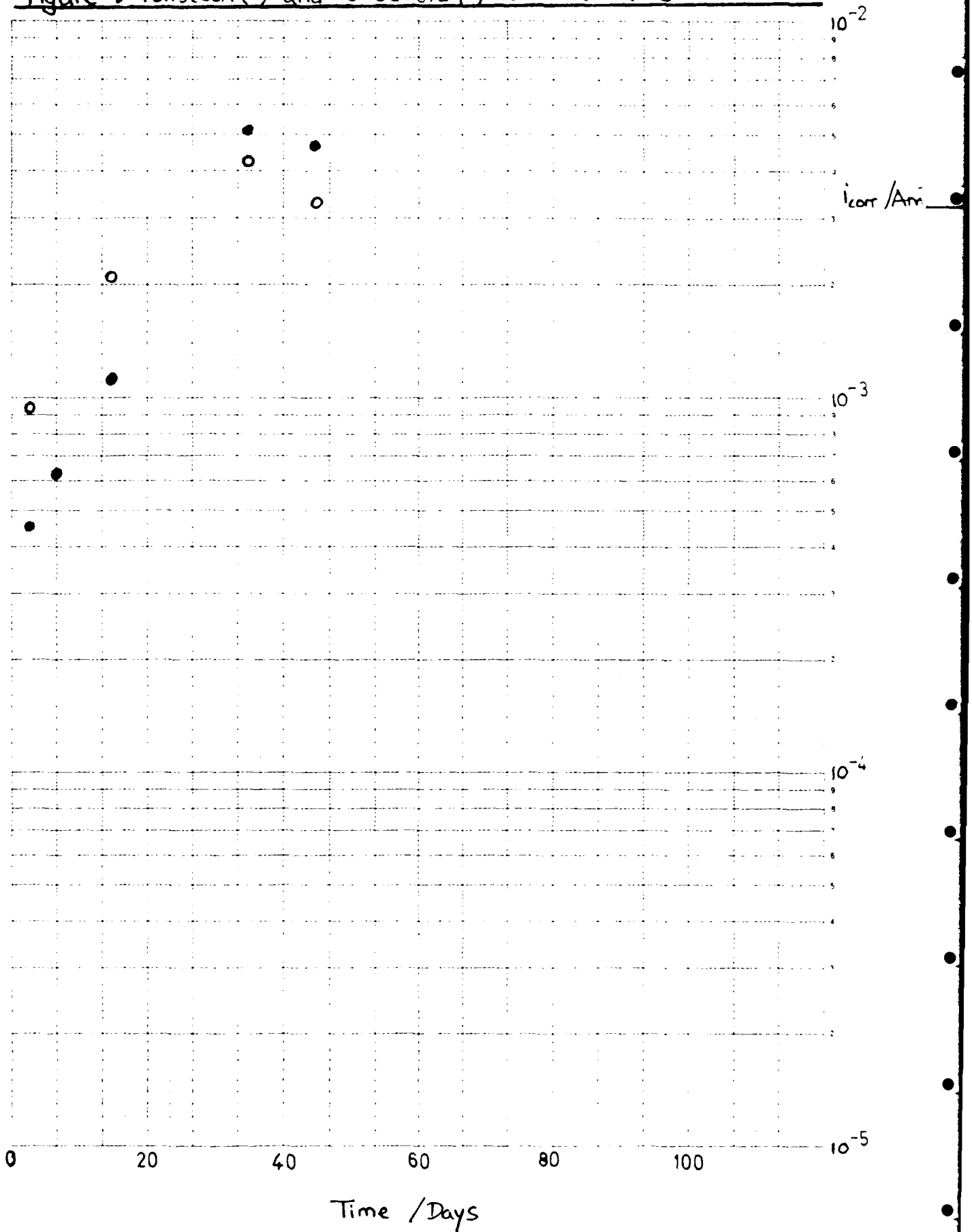

Figure 8 : AF058/1 (•) and AF058/2 (o) i_{corr} vs. time

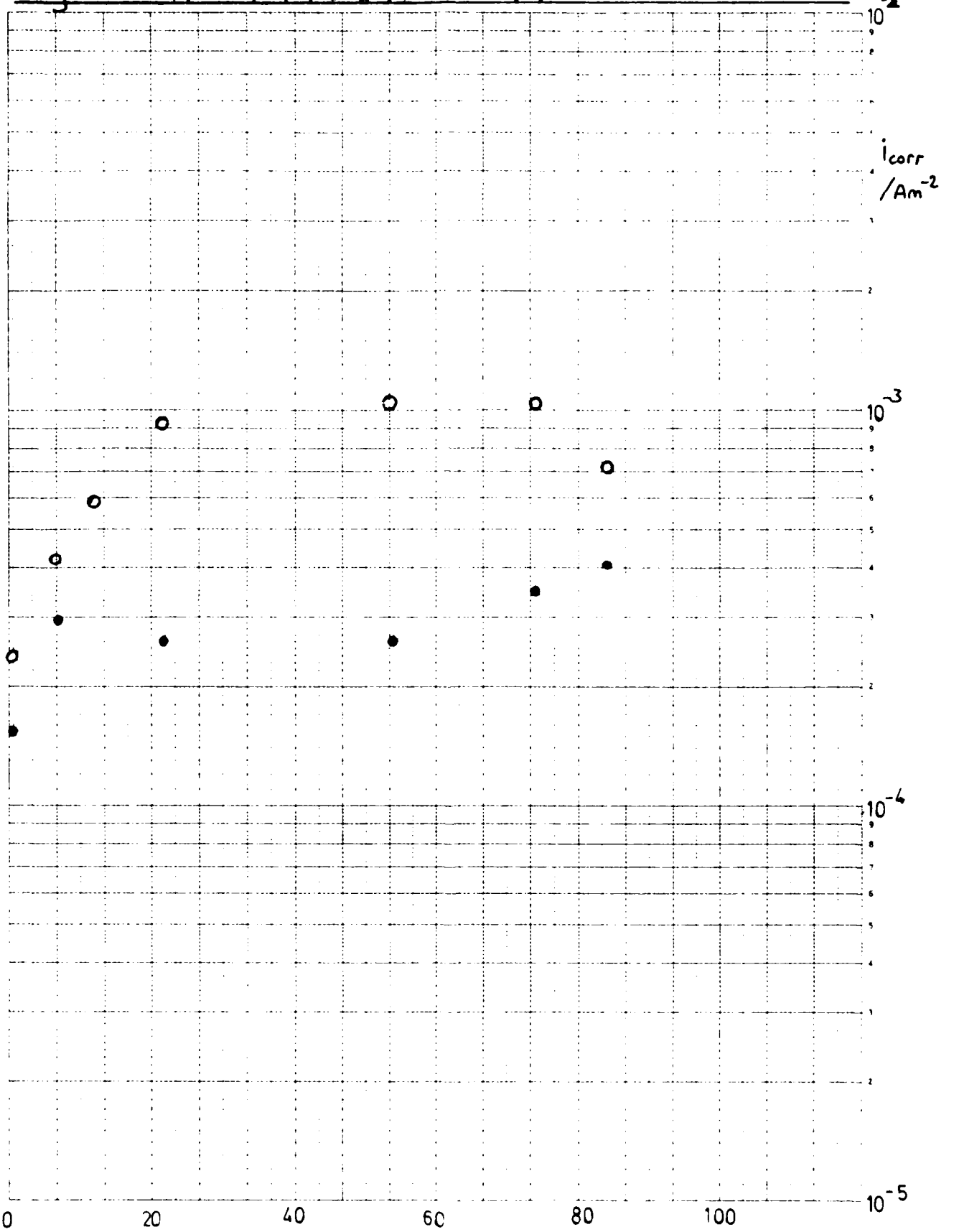

Figure 9 : W1/W2 i_{corr} versus time (• W1) (o W2)

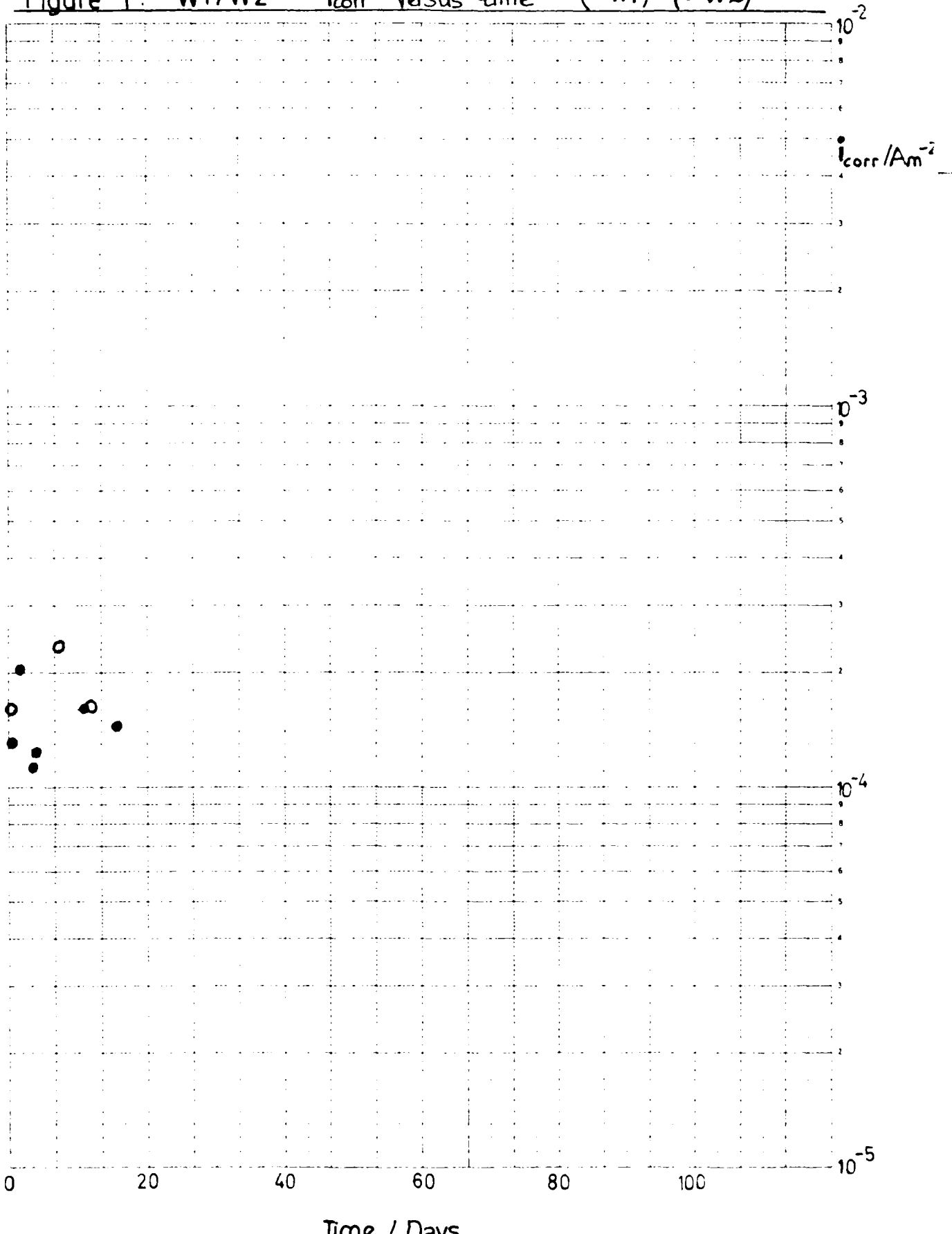

Figure 6 shows the i_{corr}-time behaviour of cells Boom1 and Boom2. Current density rises from between 2×10^{-4} Am^{-2} and 9×10^{-4} Am^{-2} to ca. 10^{-1} Am^{-2} in ca. 50 days. After this period the corrosion current density appears to stabilise at a value of ca. 1.3×10^{-1} Am^{-2}.

The i_{corr} - time data obtained from the SN5208 pair of cells, SN5208/1 and SN5208/2, and displayed graphically in figure 8, show a rapid increase in corrosion current density with time over the first 45 days. After this period the corrosion current density is ca. 4×10^{-2} Am^{-2}. These data agree closely with data reported (ref. 2, Figure 25) for the cells BW21 and BW22, which also contained IRFNA from SN5208.

Data obtained from cells AF058/1 and AF058/2 (Figure 8) again show a marked difference in behaviour between the two cells. The corrosion current density - time curve of AF058/2 is similar to those obtained for Boom 1 and Boom 2. However, the final data point plotted for AF058/2 suggests a decrease in corrosion rate not observed for the Boom cells.

Data presented for AF058/1 show a low corrosion rate Am^{-2}) for the ca first 60 days of the lifespan of this cell. After this time the corrosion rate increases to 4×10^{-1} Am^{-2} at 85 days.

Corrosion current density data for cells W1 and W2 are presented in Figure 9. Since these cells have been running for only a short time, sufficient data from which conclusions can be drawn, has not yet been

collected.

3.2)PART B - THE FOUR WORKING ELECTRODE CELL

The four working electrode cell was commissioned to investigate the effects of cell orientation on electrode behaviour. With this in mind, data has been collected with the cell in two orientations. The effect of cell orientation on corrosion is determined by observing changes in electrode behaviour when the cell orientation is altered.

Initially the cell was mounted with working electrodes 1,2 and 3 (WE1, WE2 and WE3)fully submerged in the liquid electrolyte and working electrode 4 (WE4) in the ullage space. After a time of ca. 69days the cell was rotated through 90°, so that WE4 was moved from the ullage space to the liquid phase and WE3 was moved from liquid phase to a vapour phase environment. The results of potential - time and $i_{...}$ - time measurements are presented in Figures 10 and 12 respectively. Figure 11 shows the potential-time behaviour of the four working electrodes immediately before, during and after the cell rotation through 90°.

3.2.1) Potential - Time behaviour

The data presented graphically in Figure 10 shows the typical potential - time curve already described (Section 3.1.1). It is interesting to note that data was obtained for WE4, even though this electrode was not immersed in electrolyte. Obviously a conduction pathway exists between the reference electrode and WE4 in the ullage space. This

Figure 10 Potential - Time Plot for the Four Working-electrode Cell

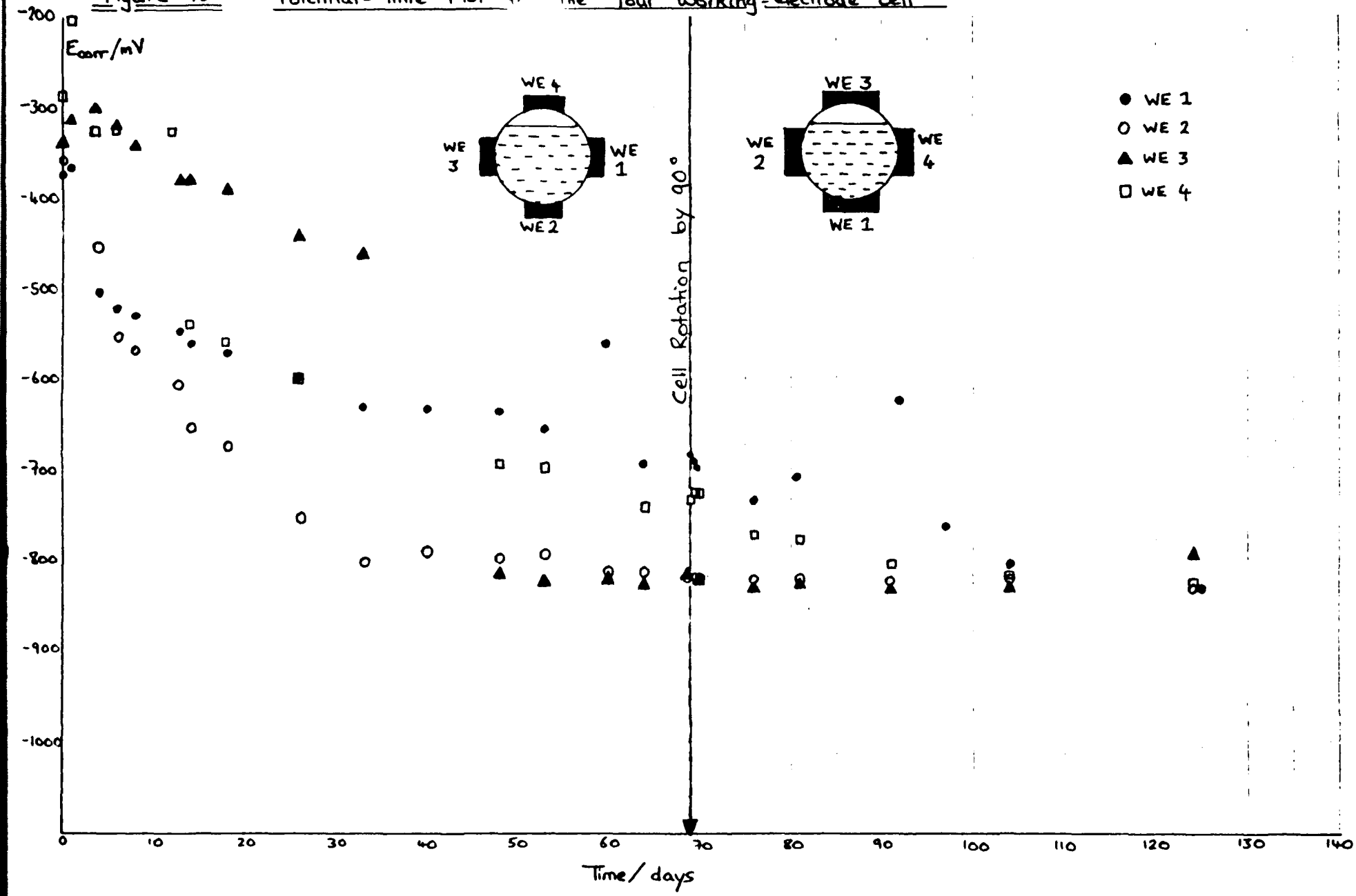

Figure 11 : Effect of Cell rotation through 90° on the corrosion potential, E_{corr}, of the four working-electrodes

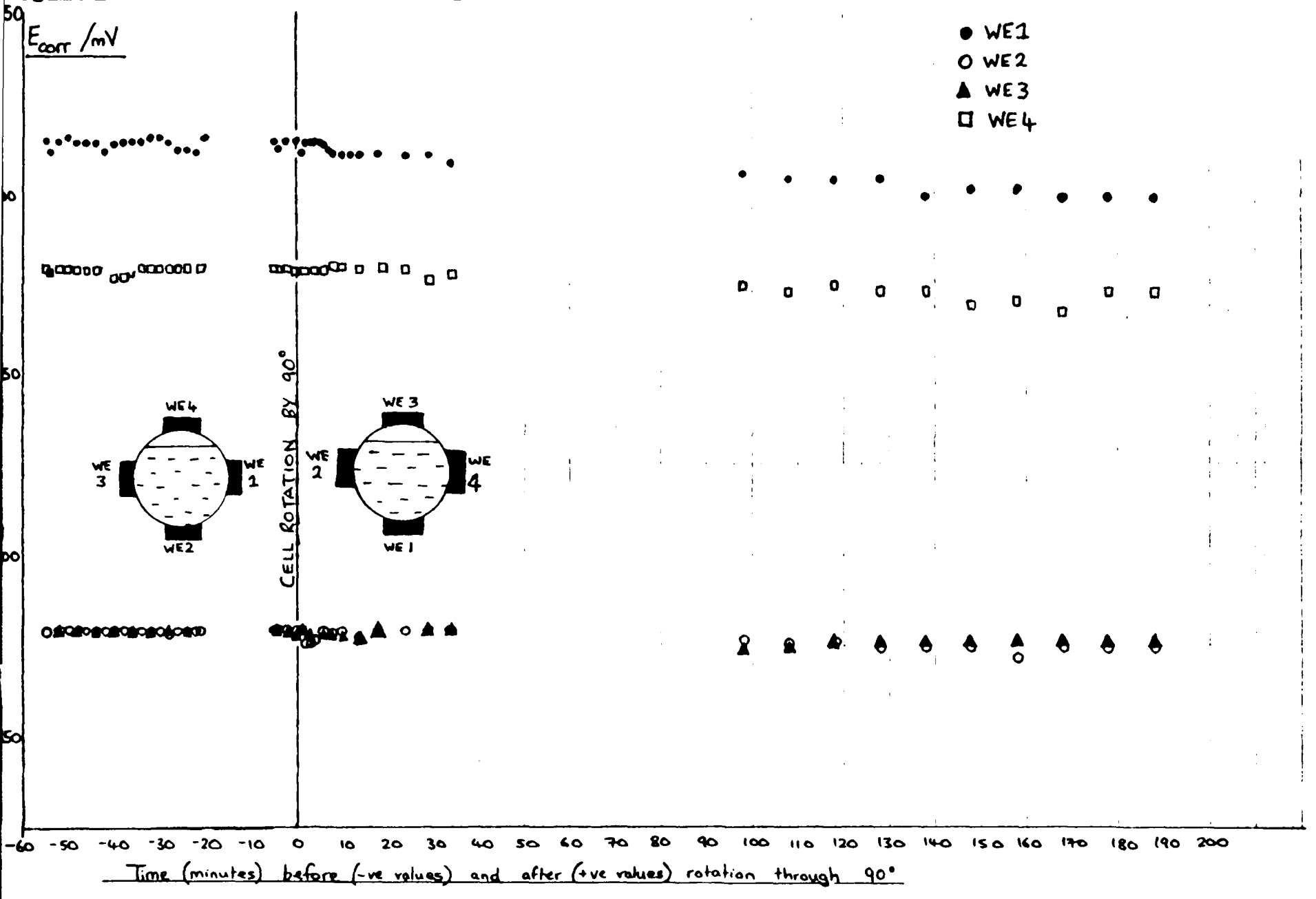

pathway exists as a result of the cell walls being wetted by electrolyte, probably during cell filling and manoeuvering in the oil-bath.

For the first ca. 33 days, WE3 showed a potential of ca. 150mV more positive (more noble) than the other liquid phase working electrodes. After 48 days, however, this potential had fallen to the value of ca. -815mV.

After a period of 69 days the cell orientation was altered by rotating the cell through 90°. Immediately prior to the rotation, and for some hours afterwards, the potentials of the four working electrodes were recorded at more frequent intervals. Figure 11 shows the potential - time behaviour of the four working electrodes during this change-over period.

Clearly, all four electrodes provided very steady potentials. Immediately after the rotation of the cell, only small potential fluctuations were observed. These consisted of decreases in potential of only ca. 5mV, and were only observed for WE1 and WE2. Three hours after cell re-orientation, no significant changes in electrode potentials had occurred.

3.2.2 Corrosion current density - Time behaviour

Figure 12 shows the corrosion current density data obtained for the four working electrode cell. At times up to the rotation point, the three working electrodes immersed in the liquid phase showed corrosion rates

Figure 12 : Four Working-electrode cell : i_{corr} vs. time

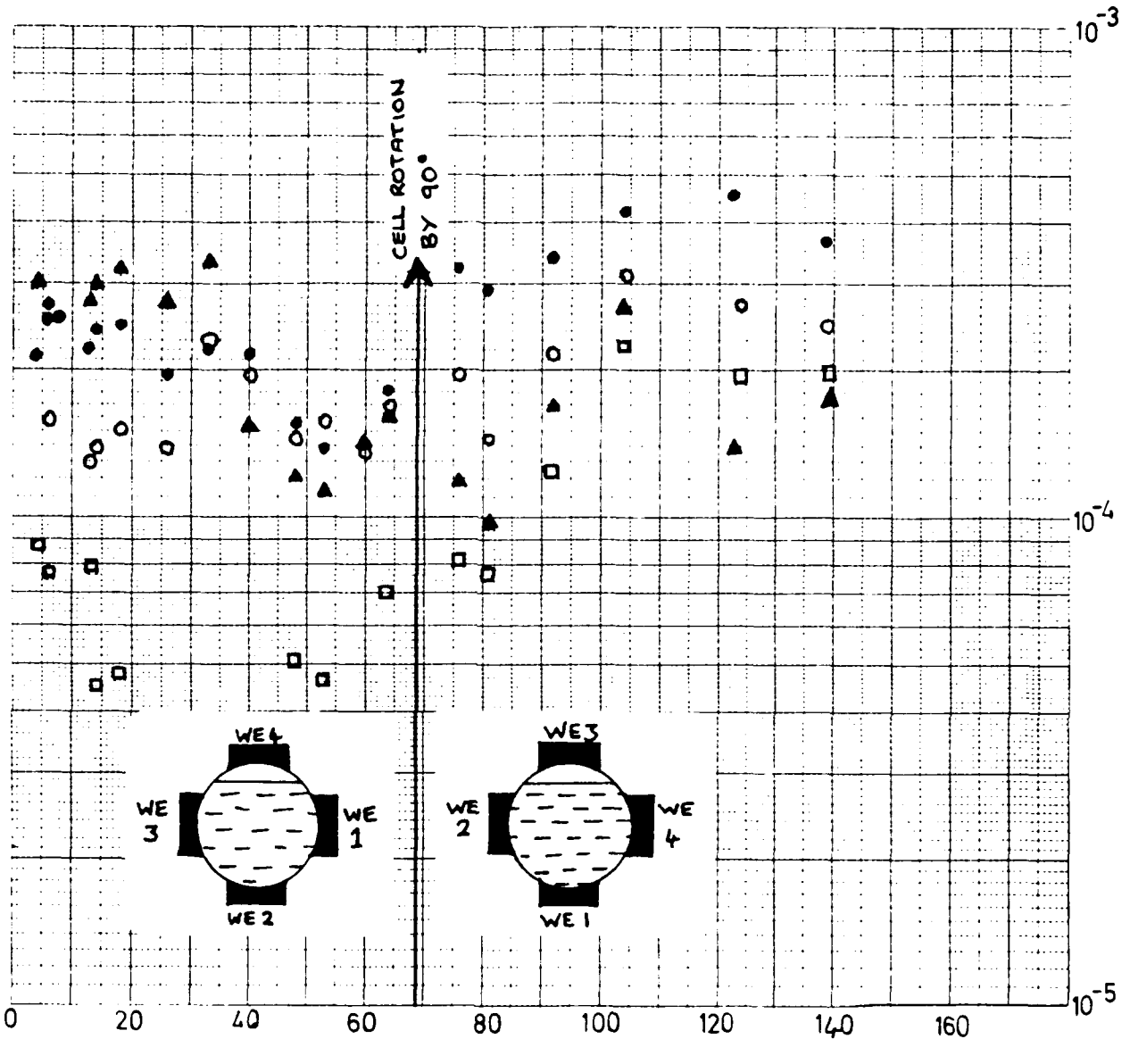

greater than those of the electrode in the ullage space (WE4). It must be pointed out, however, that without a knowledge of the degree of wetting of the surface of the ullage-space electrode, accurate corrosion current densities cannot be determined. The data displayed in Figure 12 has been calculated assuming 100% coverage of the surface of each working electrode by the IRFNA electrolyte.

Corrosion current densities of between 10^{-4} and 10^{-3} Am^{-2} are typical for these electrodes in IRFNA (BW1 and BW2B, ref. 2, Figure 15)

After rotating the cell through 90°, increases in i_{corr} were observed for all electrodes: however insufficient time has elapsed to determine whether these increases in corrosion rates will continue or whether the rates will fall to pre-rotation levels.

3.3) PART C - TEMPERATURE CYCLING

3.3.1 Procedure

The two additional cells selected for this study, BW1 and BW2B, had been set up in July and September 1986 respectively. The cells had

received no pretreatment.

Firstly the E_{corr} and i_{corr} values of the cells were obtained intermittently over the period of a week at the constant temperature of 25°C in order to determine the random fluctuations in these parameters. The results are presented in Figures 13 and 14.

The E_{corr} values of cells BW13 and BW14 were measured over a six day period whilst subjected to a series of 24 hour temperature cycles, during which the temperature was forced to oscillate between 5°C and 45°C. The results are presented in Figure 15. The structure of the cycle, shown in Figure 16, consists of a series of steps each comprising a 2 minute heating period at the rate of 1°C/min followed by a holding period of 34 minutes at the new temperature .

The four cells involved in the study (BW1, BW2B, BW13 and BW14) have now been subjected simultaneously to a 24 hour temperature cycle of identical structure to the cycle used to study the E_{corr} fluctuations of cells BW13 and BW14 during ±20°C temperature oscillations (Figure 15).

The E_{corr} and i_{corr} values for the cells were obtained at 72 minute (i.e. 4°C) intervals mid way through alternate constant temperature plateaux. No meaningful results were obtained for cell BW13 due to a short circuit between the working and counter electrodes. The short circuit has the effect of forming a galvanic couple between the aluminium and the platinum. This forces the aluminium to more anodic

FIGURE 13:

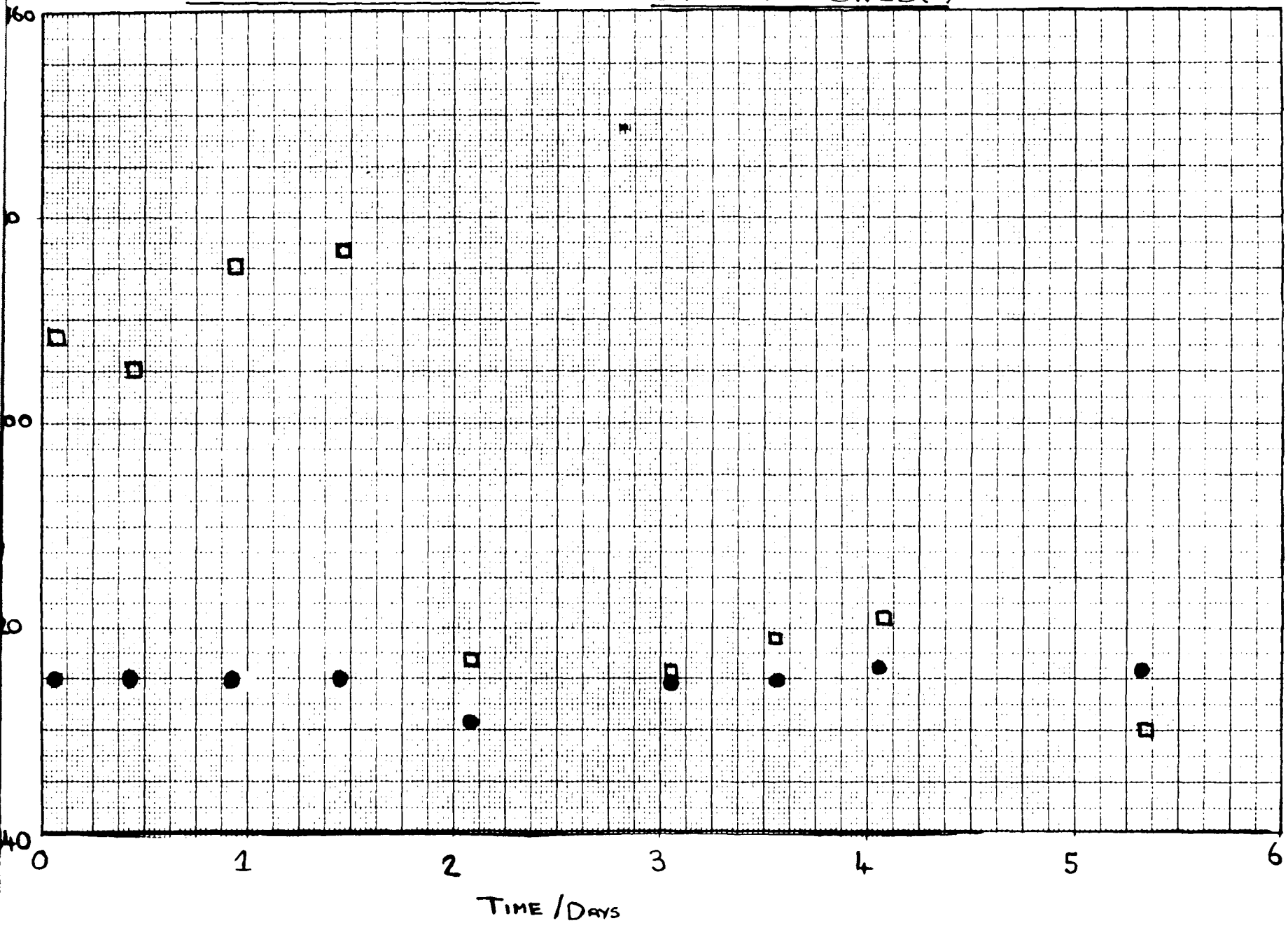
E CORR VERSUS TIME AT 25°C
BW1(□) BW2B(●)
160
0
00
0
40
0
1
2
3
4
5
6
TIME / DAYS

FIGURE 14: i_{corr} VERSUS TIME AT 25°C

BW1(□) BW2B(●)

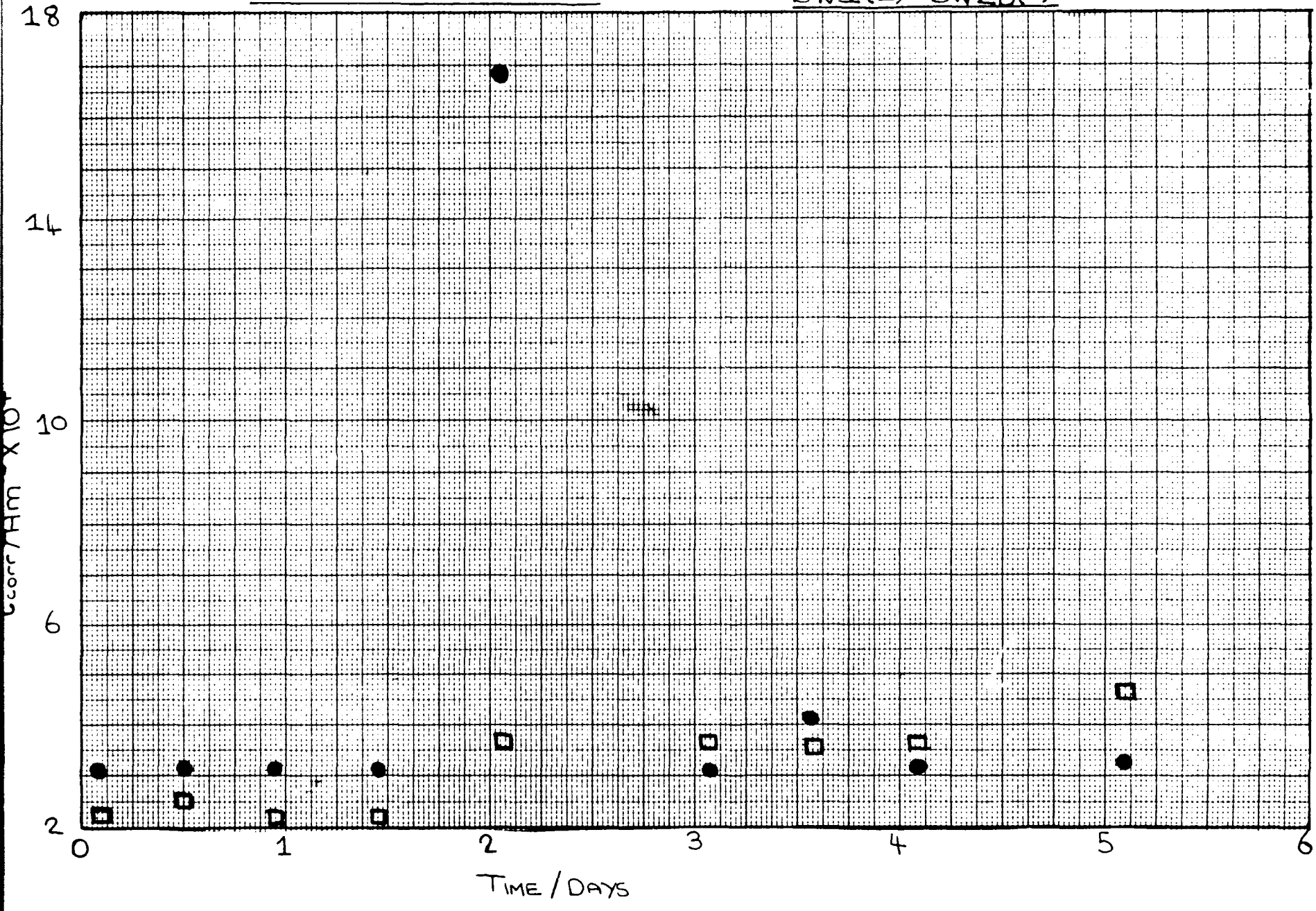

FIGURE 15:

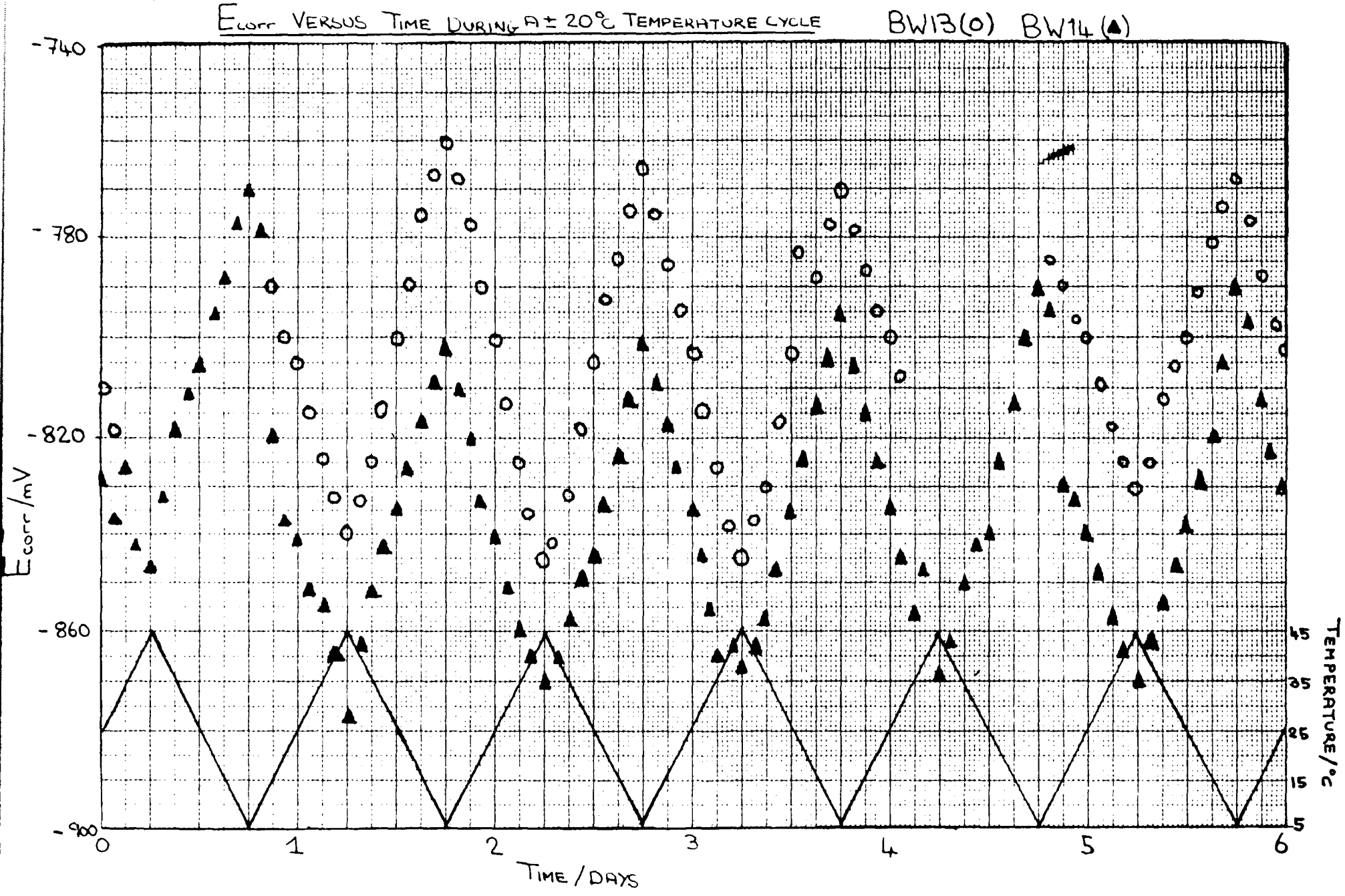
Ecorr VERSUS TIME DURING A ± 20°C TEMPERATURE CYCLE
BW13(o) BW14 (▲)
-740
-780
-820
-860
-900
Ecorr /mV
0
1
2
3
4
5
6
TIME / DAYS
45
35
25
15
5
TEMPERATURE/°C

FIGURE 16: TEMPERATURE CYCLE FOR A ± 20°C CHANGE

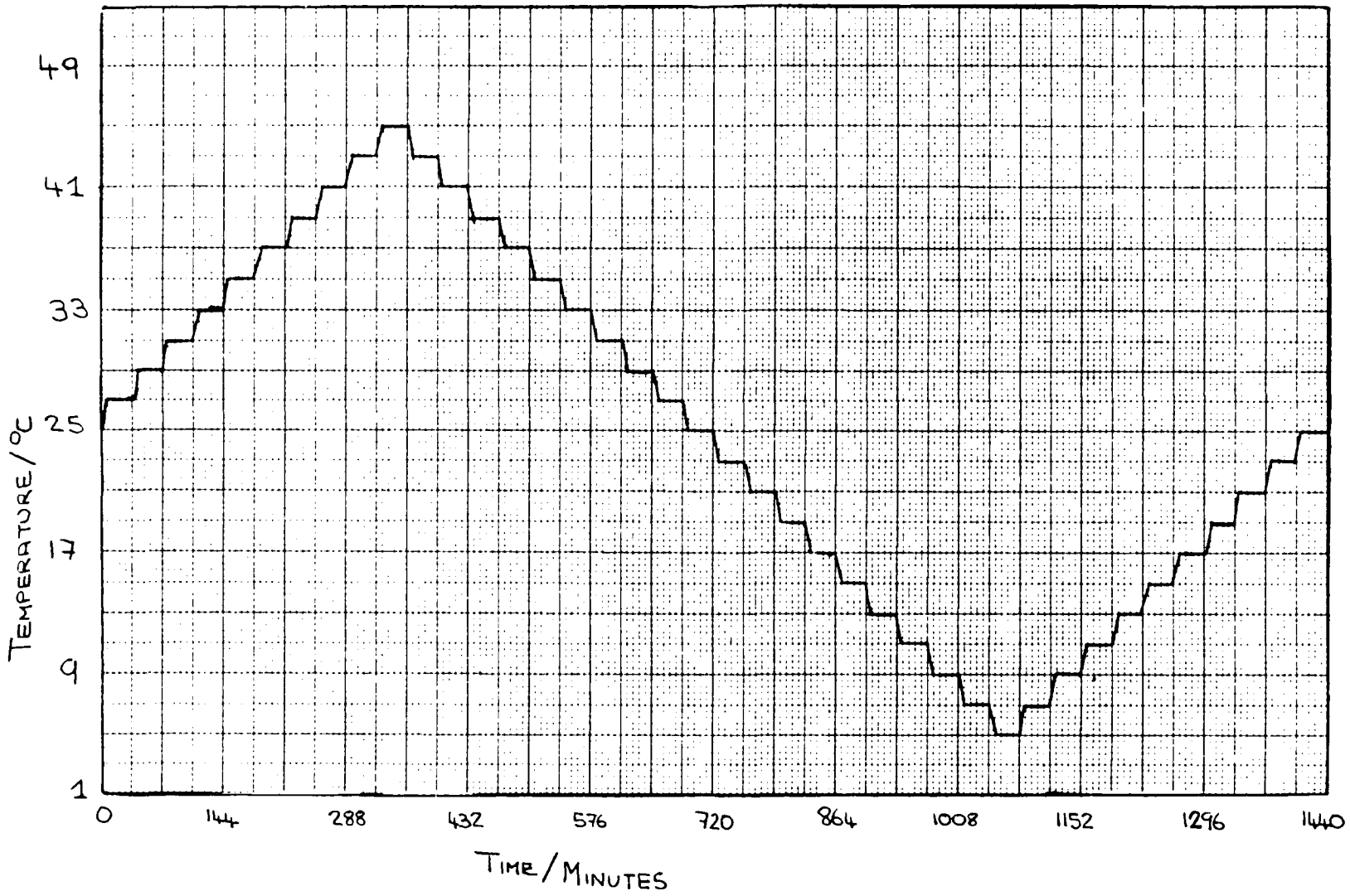

potentials, i.e. the working electrode corrodes faster. The resulting increases in E_{corr} and i_{corr} persist for many days . Hence no meaningful results could be obtained for this cell. The results for the other three cells (BW1,BW2B and BW14) are presented in Figures 17 to 22.

3.3.2) Discussion

The E_{corr} and i_{corr} measurements made on the cells BW1 and BW2B thermostatted at 25°C were found to be essentially time independent as was previously shown for the cells BW13 and BW14 thermostatted at 25°C (ref. 1, Figures 3 and 4). For the cell BW1 the E_{corr} and i_{corr} values concurred within 30mV and $2x10^{-4}Am^{-2}$, respectively. For the cell BW2B the agreement was within 10mV and $1x10^{-4}Am^{-2}$ (apart from one rogue result).

The E_{corr} and i_{corr} values measured during the 24 hour cycle show a clear cyclic variation with time (Figures 15 and 17-22). One feature of the cyclic varation is the apparent 'reversibility' of the changes caused by the temperature oscillation; on no occasion has any hysteresis been observed. The cyclic variation of the i_{corr} values is not, however, symmetrical (Figures 17,19 and 21). This feature was not detected during the ±5°C temperature cycle (ref. 1, Figure 8). The results show disproportionately high values of i_{corr} at the higher temperatures. In order to quantify this effect it is valuable to look at

FIGURE 17:

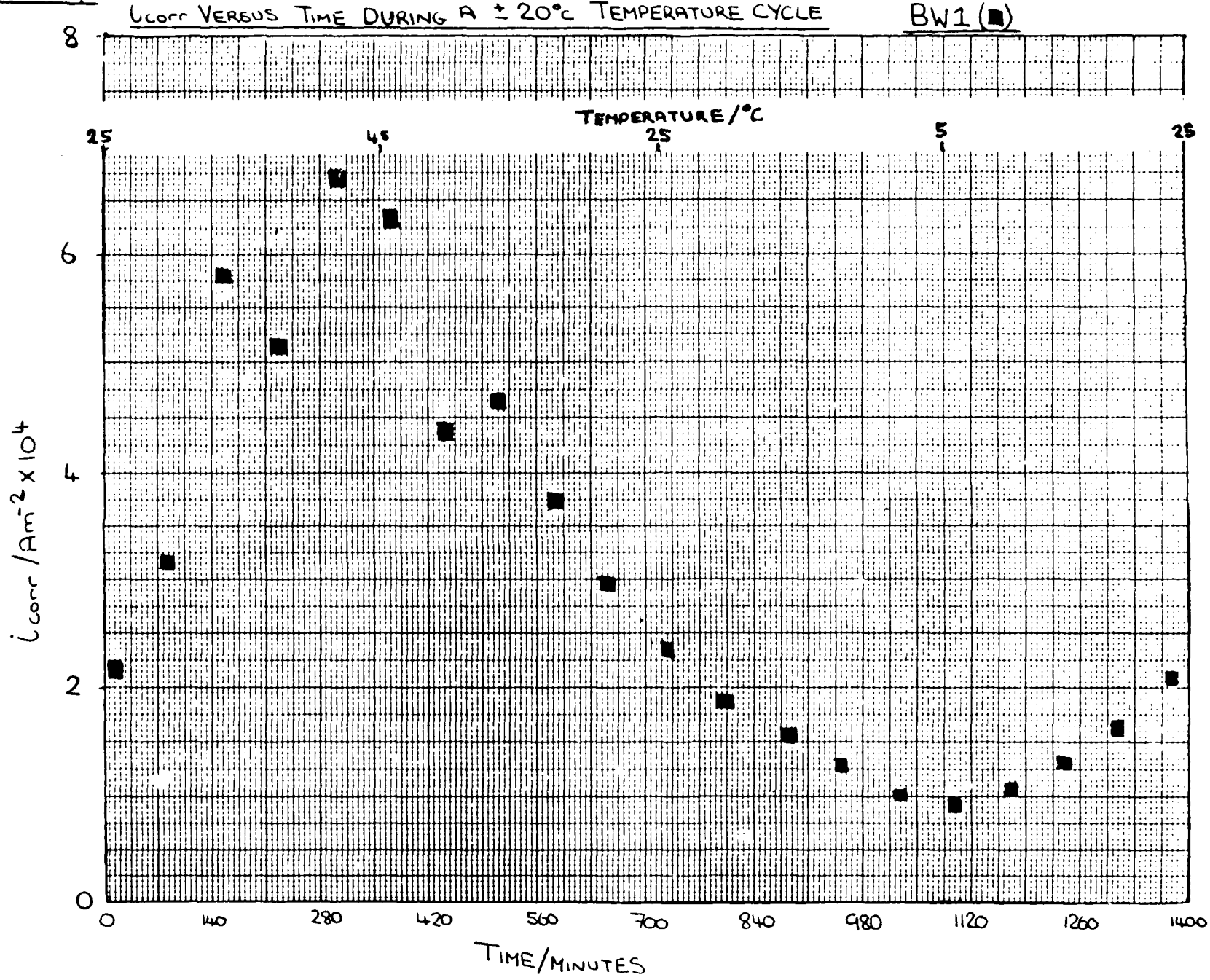
i_{corr} VERSUS TIME DURING A ± 20°C TEMPERATURE CYCLE
BW1 (■)
TEMPERATURE/°C
25
45
25
5
25
8
6
4
2
0
i_{corr} /Am^{-2} x 10^4
0
140
280
420
560
700
840
980
1120
1260
1400
TIME/MINUTES

FIGURE 18:

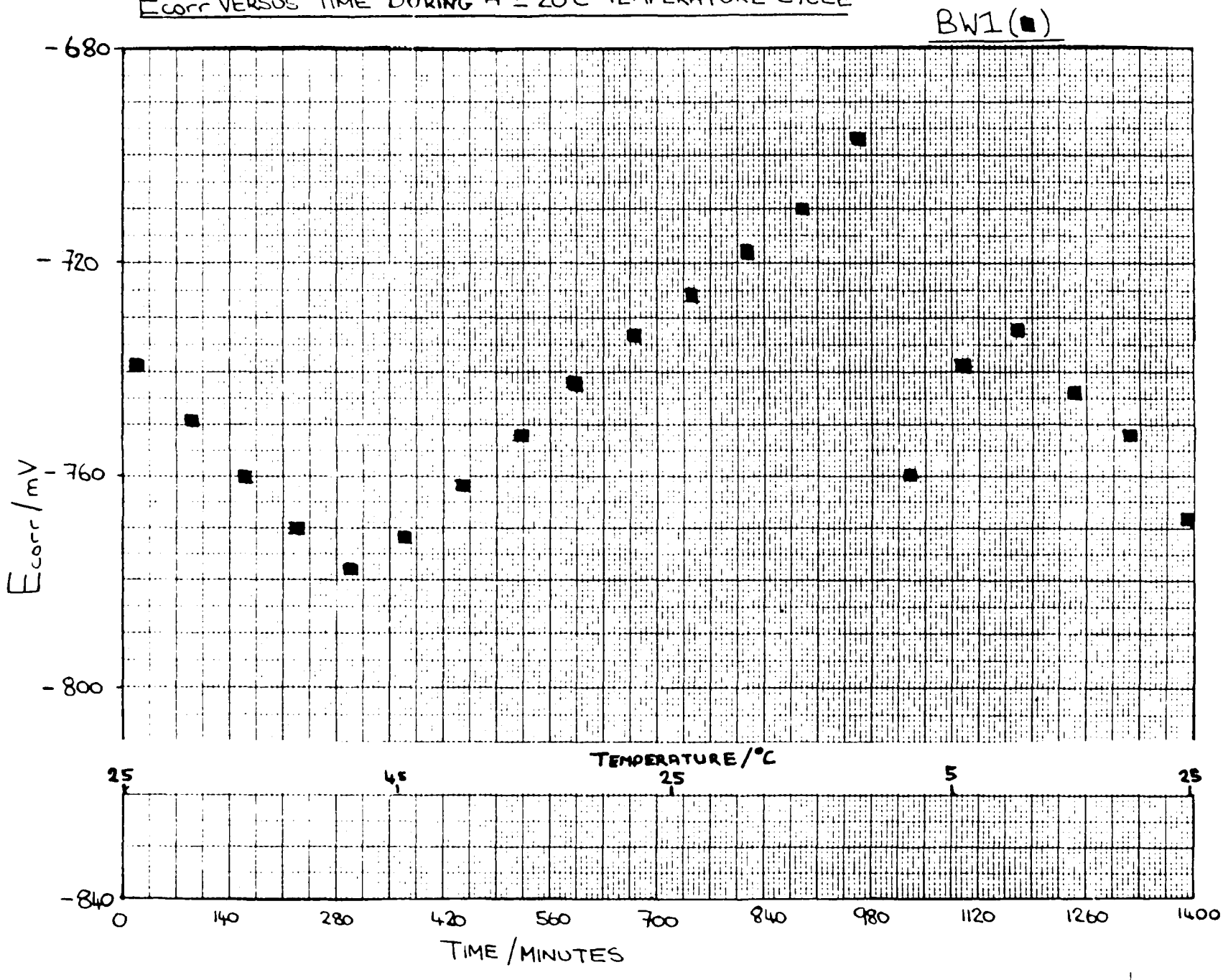
Ecorr VERSUS TIME DURING A ± 20°C TEMPERATURE CYCLE
BW1 (■)
-680
-720
-760
-800
-840
Ecorr / mV
TEMPERATURE / °C
25
45
25
5
25
0
140
280
420
560
700
840
980
1120
1260
1400
TIME / MINUTES

FIGURE 19:

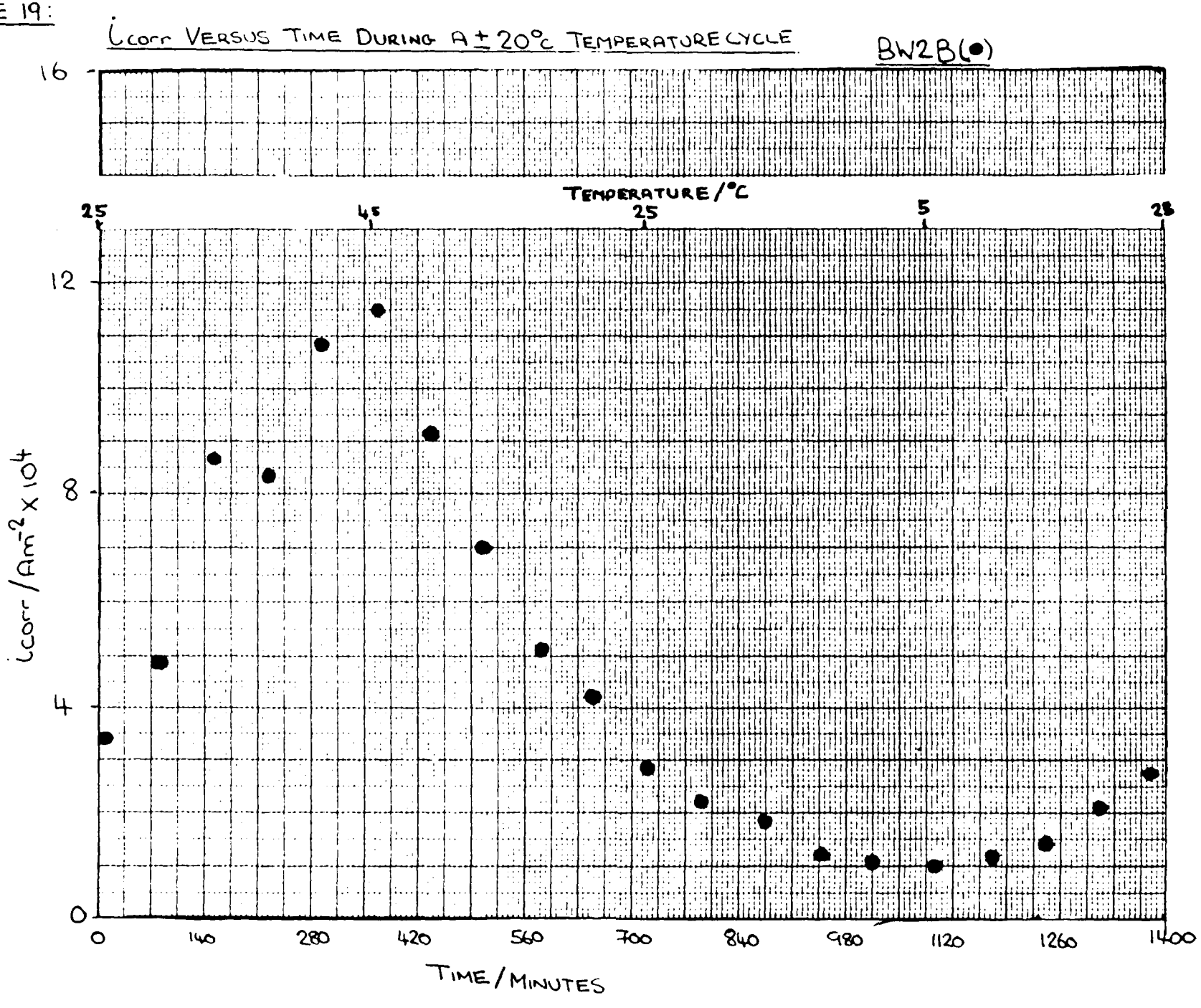
i_{corr} VERSUS TIME DURING A ± 20°C TEMPERATURE CYCLE
BW2B(●)
TEMPERATURE/°C
25
45
25
5
25
16
12
8
4
0
i_{corr} /Am^{-2} x 10^4
0
140
280
420
560
700
840
980
1120
1260
1400
TIME/MINUTES

FIGURE 20:

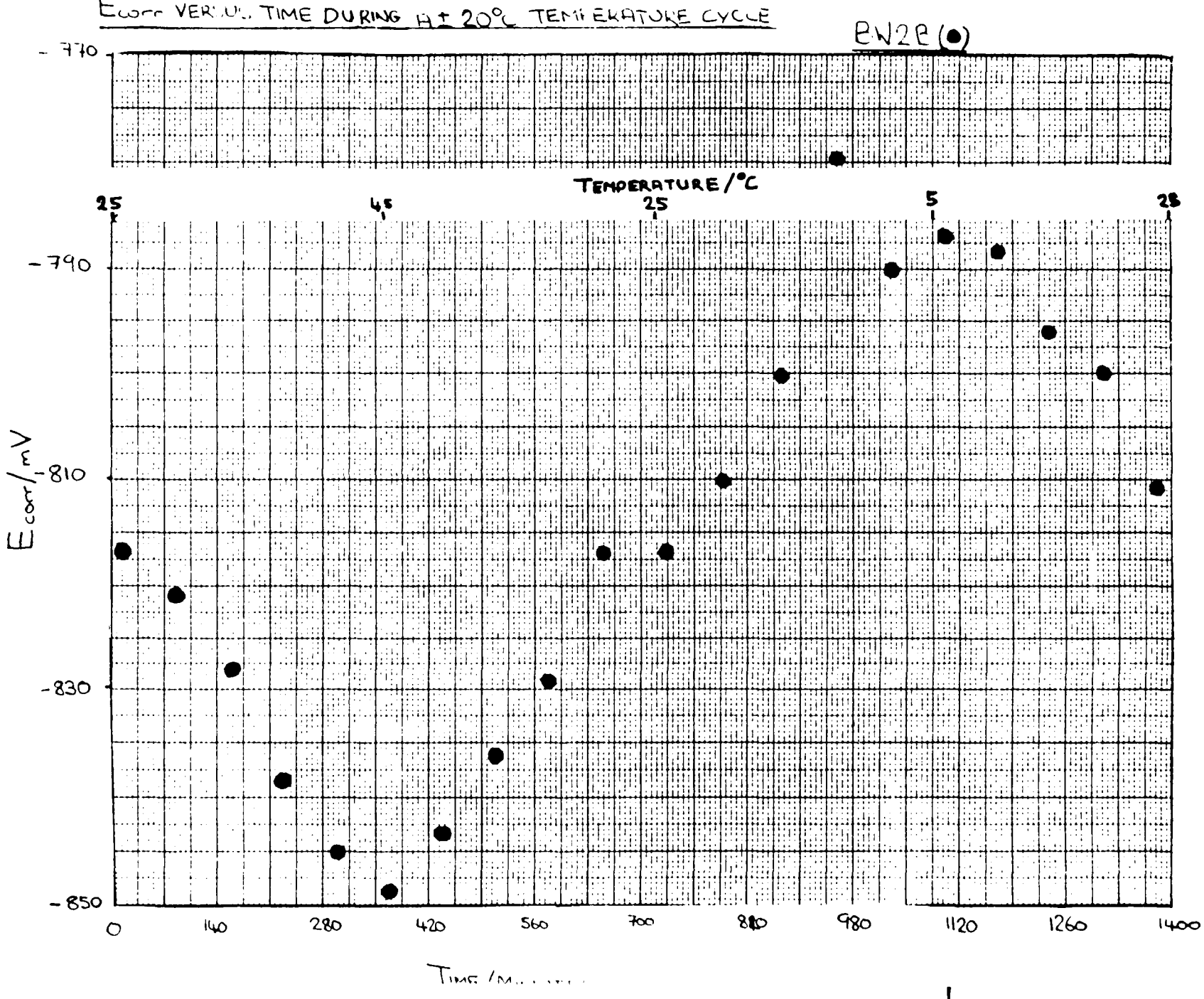
E_{corr} VERSUS TIME DURING A ± 20°C TEMPERATURE CYCLE
BW2B (●)
-770
TEMPERATURE /°C
25
45
25
5
25
-790
-810
-830
-850
E_{corr} / mV
0
140
280
420
560
700
840
980
1120
1260
1400
TIME /

FIGURE 21: i_{corr} VERSUS TIME DURING A ± 20°C TEMPERATURE CYCLE BW14(▲)

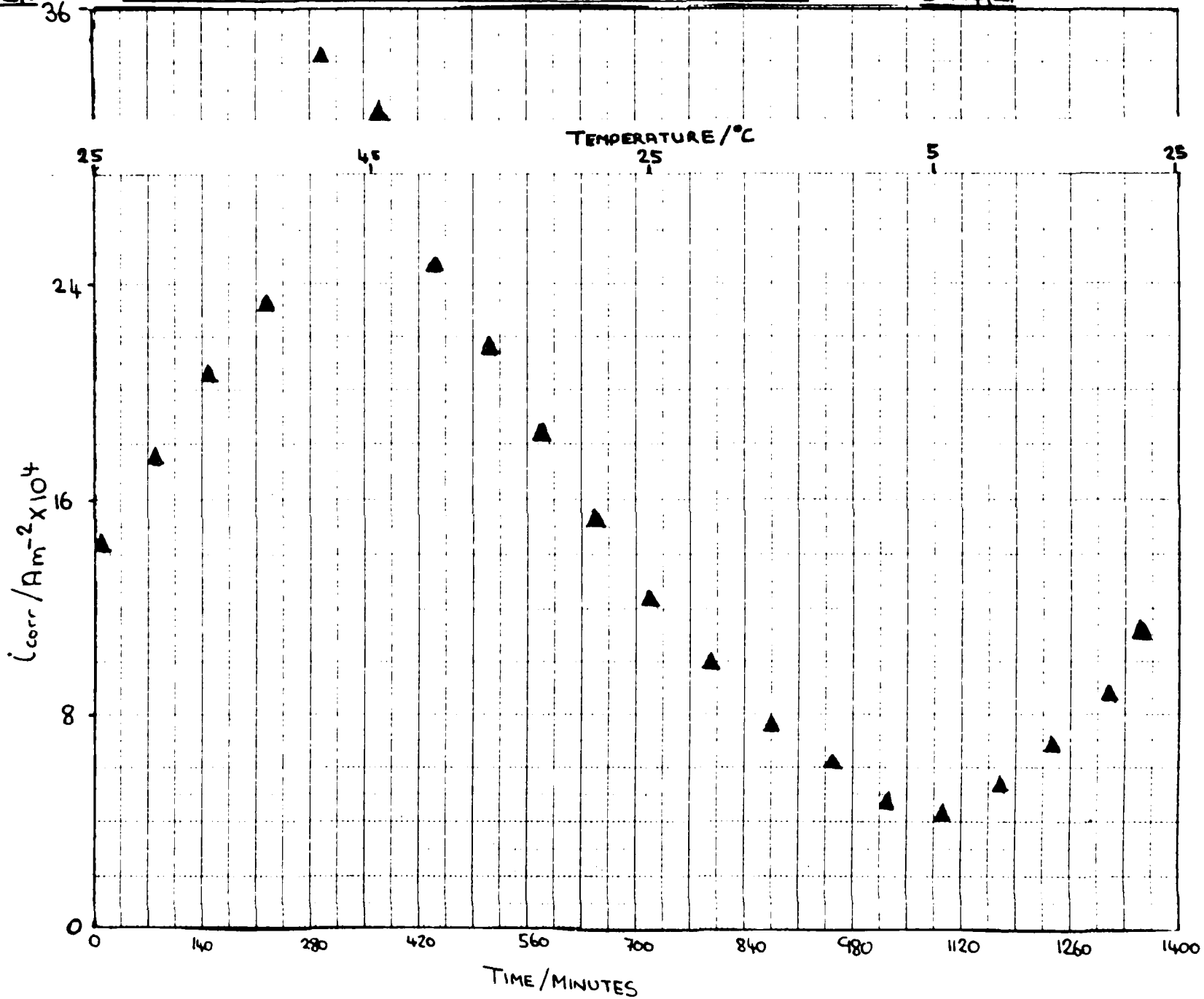

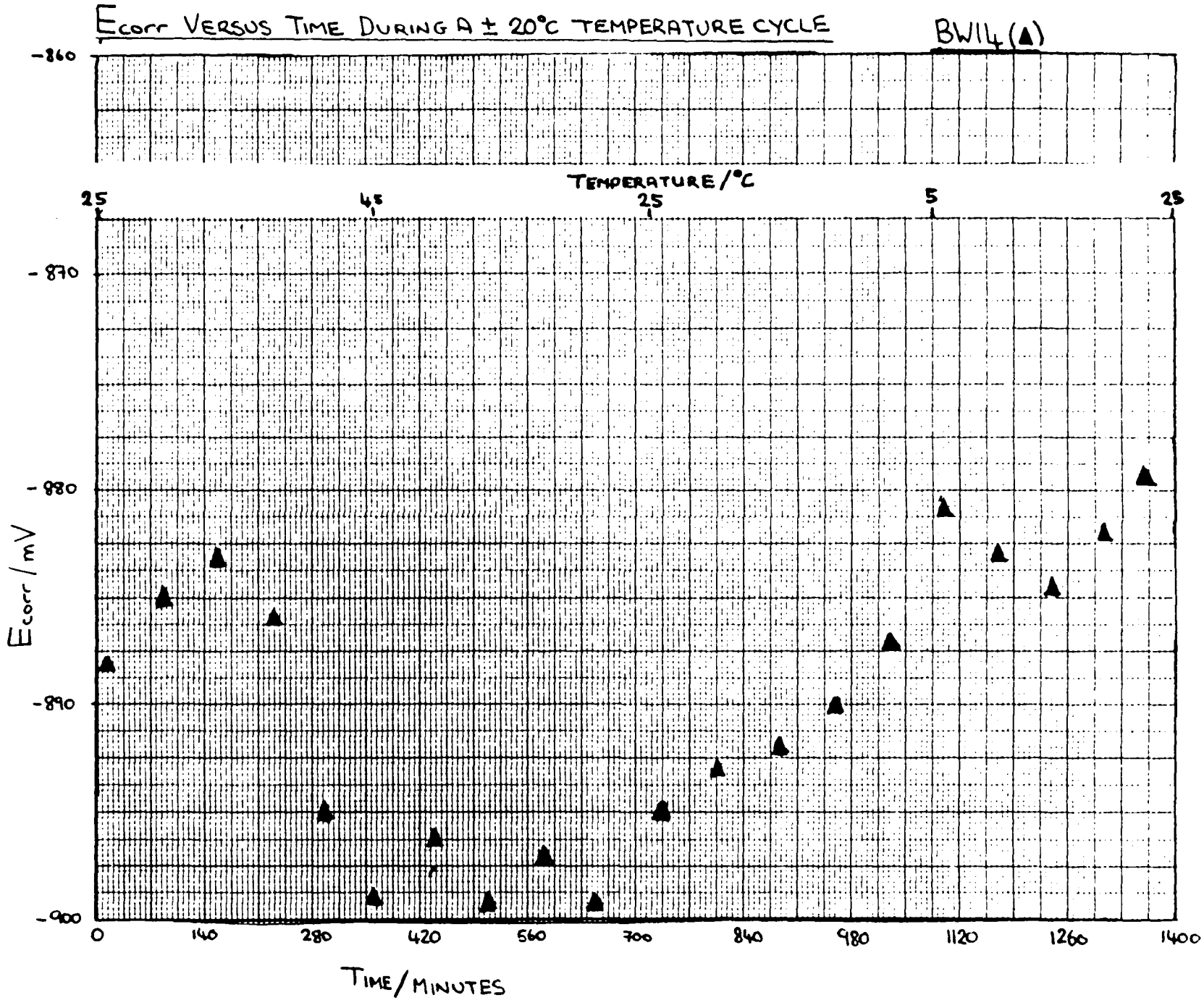
Ecorr VERSUS TIME DURING A ± 20°C TEMPERATURE CYCLE
BW14 (▲)
-860
TEMPERATURE/°C
25
45
25
5
25
-870
-880
-890
-900
Ecorr / mV
0
140
280
420
560
700
840
980
1120
1260
1400
TIME/MINUTES

some average i_{corr} values (Table 3.1).

The mid-cycle i_{corr} value is the value after 12 hours of the 24hour cycle when the temperature returns to 25°C. Comparing the mid-cycle values with the mean i_{corr} values during the 24 hour cycle leads to the conclusion that the effect of the temperature oscillation is to produce an increase in corrosion rate of between 15% and 35% relative to the thermostatic corrosion rate (at 25°C).

TABLE 3.1: i_{corr} values

Cell Code	Mean i_{corr} ±20°Cycle	Mean i_{corr} at 25°C	Mid-cycle i_{corr} at 25°C
BW1	$3.01 \times 10^{-4} Am^{-2}$	$3.16 \times 10^{-4} Am^{-2}$	$2.60 \times 10^{-4} Am^{-2}$
BW2B	$4.56 \times 10^{-4} Am^{-2}$	$4.40 \times 10^{-2} Am^{-2}$	$3.40 \times 10^{-4} Am^{-2}$
BW14	$1.50 \times 10^{-4} Am^{-2}$	$5.12 \times 10^{-2} Am^{-2}$	$1.31 \times 10^{-4} Am^{-2}$

The comparison between the mean i_{corr} values during the 24 hour cycle and those recorded at the constant temperature (25°C) is less

informative . There are two main reasons for this: firstly, a few atypical points may cause a large change in the mean i_{corr} value and secondly, natural drift in i_{corr} in the period between measuring the thermostatic values and commencing the temperature cycle. The first point is especially important for BW2B (Figures 14 and 19) where a comparison of the mean i_{corr} value during the ± 20°C cycle with the median value of i_{corr} at 25°C ($3.15 \times 10^{-4} Am^{-2}$) shows a 31% increase in the corrosion rate, consistent with the above conclusion. However, a similar comparison with the mean i_{corr} value at 25°C would clearly be invalidated by the single rogue point. The second point is important for both BW1 and BW14 and a further set of confirmatory readings at 25°C will be recorded for these cells.

The i_{corr} data for each cell show an exponential variation with absolute temperature , i.e. fit the Arrhenius equation:-

$$\text{Rate} \propto i_{corr} = A\exp^{(-E_a/RT)}$$

A = Arrhenius constant

E_a = Activation energy ($kJmol^{-1}$)

R = Gas constant = $8.31 JK^{-1}mol^{-1}$

T = Temperature (K)

Hence by plotting i_{corr} against 1/T and using an exponential

regression analysis to obtain the best curve fit, values of A and E_a have been obtained (Table 3.2).

TABLE 3.2: Arrhenius parameters

Cell Code	Arrhenius Constant	Activation Energy ($kJmol^{-1}$)	Correlation Coefficient
BW1	2.2×10^{3}	39.6	0.964
BW2B	2.7×10^{5}	50.6	0.983
BW14	9.2×10^{3}	39.1	0.993

A final observation arising from the ±20°C temperature cycle is that the E_{corr} and i_{corr} data are much less capricious than those observed during the ±5°C 24-hour cycle (ref.1, Figures 7 and 8). Data for the ±5°C cycles were recorded using the PARC Model 273 potentiostat, whereas data for the ±20°C cycle were obtained using a Thompson Autostat Model 251 potentiostat. This has led to the conclusion that some of the 'spikes' seen in the ±5°C cycle may have been instrumental in origin.

In conclusion the temperature oscillation produces an exponential reversible fluctuation in the corrosion rate . In consequence of this it is suggested that, in order to minimise the corrosion of the oxidiser tanks, a storage site should be selected in a cool climate with a minimum fluctuation in temperature .

3.4) PART D - SURFACE STUDIES

The proposal is to study five pairs of samples cut from oxidiser tank SN5144. The pretreatments agreed are as follows:

1) No pretreatment
2) H_2O wash, dry
3) H_2O wash, dry, IRFNA (3 months)
4) H_2O wash, dry, HF/F_2
5) H_2O wash, dry, HF/F_2, IRFNA (3months)

For sample pairs 3 and 5, the final stage of the pretreatment involving immersion in IRFNA (R.O. Westcott Lot67 Drum3) was commenced on 25 May 1988. All the samples will be characterised using the Auger facility at Loughborough Consultants Ltd. when the three month exposure period of these two pairs of samples is complete.

3.5) PART E - "DOPING"

The addition of water to IRFNA in order to assess its effect upon corrosion rates has met with some technical problems.

It was initially proposed to adjust the water content of the IRFNA in electrochemical cells by injecting into those cells small quantities of RFNA to which known amounts of water had been added. Unfortunately we have been unable to obtain reliable and reproducible values for the initial water content of IRFNA samples (Section 3.6.3) and so have been unable as yet to obtain data on the effects of water content on corrosion rates by this method.

3.6) IRFNA ANALYSES

3.6.1) Total solids

Total solids determinations were performed according to the method outlined in the U.S Army laboratory analysis standard for IRFNA (Dated April 1987, ref. 3). The values so far obtained are recorded in Table 3.3. Sets of determinations will also be carried out the other samples of IRFNA supplied.

Table 3.3: Total solids content of IRFNA samples

IRFNA Sample	Solids Content / wt*
Lot67 Drum3	0.091
	0.194
	0.134
Boom	0.071
	0.046
	0.049
	0.064

* as metallic nitrate (ref. 3).

3.6.2 HF content

The HF inhibitor content of IRFNA samples was determined as reported previously (ref. 2). Table 3.4 lists the results obtained.

TABLE 3.4: HF content of IRFNA samples

IRFNA Sample	HF Content / wt%
Westcott lot67 / drum3	0.519
SN5208	0.576
AF175	0.592
AF058	0.471
Boom	0.519
"New" Westcott	0.559

It should be noted that IRFNA from the "new" Westcott and AF175 batches has not been used in this research project.

3.6.3) H_2O Content

The water content of IRFNA is determined from the near infra-red absorption spectrum of the sample between 1500 and 1350 mμ (nm) versus CCl_4. both contained in 5mm path length cells as described in ref. 4.

Unfortunately we have been unable to obtain consistent and reproducible values for the water content of IRFNA samples. This is partly due to losses of sample from the infra-red cell through leakage during scanning. Further losses occur as a result of evaporation of sample in the heat of the IR beam. This latter problem can be greatly reduced by increasing the scan rate though this will lead to a lower sensitivity.

We are at present looking at ways of overcoming these technical problems.

3.6.4) Metals Content

At the present time metals content analyses have been carried out on two batches of IRFNA (SN5208 and "new" Westcott). The results of these analyses are presented in Table 3.5.

Table 3.5: Metals content of IRFNA samples

IRFNA batch	Metal concentration / ppm Al	Cu	Fe	Cr	Ni
"New" Westcott	200.2	1.9	-	65.0	39.5
SN5208	180.6	8.8	11.5	34.1	0.5
Lot67 Drum3	101.5	1.8	-	34.9	31.2
AF175	194.1	1.1	7.5	1.6	0.5
AF058	205.0	1.1	6.8	1.7	ND
BOOM	147.6	7.0	6.5	0.9	0.4

4) REFERENCES

1) M.F.A.Dove, N.Logan, J.F.Richings and J.P.Mauger
Corrosion of Aluminium Alloys by IRFNA, March 1988.
RD 5878-CH-01

2) M.F.A.Dove, N.Logan and J.F.Richings
The Investigation of Corrosion Rates of Lance Aluminium Alloys by Inhibited Red Fuming Nitric Acid (IRFNA).
Final Report, July 1987.

3) Laboratory Analysis Standard for Inhibited Red Fuming Nitric Acid (IRFNA). Research, Development and Engineering Center, Propulsion Directorate, Redstone Arsenal, Alabama.

4) MIL-P-7254F (30 April 1970): Military Specification: Propellants, Nitric Acid.